DEVELOPMENT OF AN INSULATION PLASTER FOR FIBER REINFORCED POLYMER (FRP) CONCRETE COMPOSITES USING CEMENTITIOUS MATERIAL

S.Kajanan

198024A

Degree of Master of Science

Department of Civil Engineering

University of Moratuwa

Sri Lanka

January 2021

DEVELOPMENT OF AN INSULATION PLASTER FOR FIBER REINFORCED POLYMER (FRP) CONCRETE COMPOSITES USING CEMENTITIOUS MATERIAL

S.Kajanan

198024A

Thesis submitted in partial fulfillment of the requirements for the degree Master of Science in Civil Engineering

Department of Civil Engineering

University of Moratuwa

Sri Lanka

January 2021

DECLARATION

I declare that this is my own work and this thesis does not incorporate without acknowledgement any material previously submitted for a Degree or Diploma in any other university or institute of higher learning and to the best of my knowledge and belief it does not contain any material previously published or written by another person except where the acknowledgement is made in the text.

Also, I hereby grant to University of Moratuwa the non-exclusive right to reproduce and distribute the thesis, in whole or in part in print, electronic, or other media. I retain the right to use this content in whole or part in future works (such as articles or books).

Signature: Date: 11/01/2021

The above candidate has carried out the research for Masters under my supervision

Name of the supervisor: Dr. (Mrs.) J.C.P.H. Gamage

Signature of the supervisor: Date:

Name of the supervisor: Dr. G.I.P. De Silva

Signature of the supervisor: Date:

ACKNOWLEDGEMENT

This research addresses one of the main concerns of the civil engineering industry when it comes to Fibre Reinforced Polymer Composites. The knowledge I gained through my undergraduate work and postgraduate studies has been a great influence in completing this project up to the standards.

There are many individuals to whom I owe this success to. Foremost, I would like to acknowledge my research supervisors, **Dr.(Mrs.) J.C.P.H. Gamage**. Senior Lecturer, Department of Civil Engineering, University of Moratuwa, and **Dr. G.I.P. De Silva**. Senior Lecturer, Department of Materials Science and Engineering, University of Moratuwa. Neither of these would be possible without their guidance.

Next, I would like to thank **Dr.(Mrs.) H.L.D.M.A. Judith**. Chairman, Research and Development Division, Road Development Authority, Chairperson of my Research Assessment Panel, and **Prof. A.A.D.J. Perera**. Senior Professor, Department of Civil Engineering, University of Moratuwa. Research coordinator (Nominee) for evaluating and guiding throughout the research progress presentations.

I would like to appreciate the financial support of the project from the National Research Council, Sri Lanka, and Airow Solutions (Pvt.) Ltd. (Grant No. PPP18-01). Especially, **Mrs. Naduni Wanniarachchi**. Scientific Officer, National Research Council, and **Mr. Vajira Attanayake**. General Manager, Airow Solutions (Pvt.) LA. for their assistance.

Moreover, I would like to express my gratitude to Mr**. D.M.N.L. Dissanayaka** of Structural Testing Laboratory and **Mr. H.T.R.M. Thanthirige** of Building Materials Laboratory, University of Moratuwa for their support, throughout the experimental works. Last but not least, I want to thank my parents and family for believing in me and encouraging me throughout these years.

S.Kajanan
Department of Civil Engineering
University of Moratuwa
11.01.2021

ABSTRACT

The energy used to maintain the thermal comfort of building greatly contributes the greenhouse gas (GHG) emissions and global warming. This study developed a sustainable cost-effective rice husk ash (RHA) based mortar for the wall plaster to improve the thermal insulation, reduce the operational energy and enable the thermal comfort. RHA was partially replaced the sand in the conventional mortar to produce the RHA based plaster. Compressive strength and thermal conductivity tests were conducted, and the results highlight that the RHA can be replaced up to 30% of sand in the conventional mortar to produce a wall plaster with improved thermal insulation with adequate compressive strength. Further, this study investigates the thermal performance of the RHA-based plaster through measured the heat transfer rate under full open weather conditions. Two identical prototype model houses were constructed with RHA-based plaster and conventional plaster, and internal and external wall surface temperatures were measured for 3-days cycles. The results highlighted that on average peak heat flux reduction formed by the RHA-based plaster mortar was 10%. The average daily heat transfer reduction across the wall with RHA-based plaster was 26%. Further, results show that RHA-based plaster can reduce the energy that required to enable the thermal comfort by about 9% than the conventional mortar. The environmental impact analysis was also conducted to assess the sustainable performance of RHA-based mortar. The assessment highlights that RHA-based mortar has less environmental impact than the conventional mortar. Further, the CO_2 emission produced by the production of RHA-based mortar is about 14% less than that of from conventional mortar. At last stage the developed plaster was applied with CFRP specimens and checked for the thermal test and bond test using single shear test. 70% to 73% fire resistance can be achieved respect to the commercially available material (Vermiculite-cement).

Keywords: Plaster; Rice Husk Ash; Thermal properties; Life cycle Assessment; Compressive strength; Heat transfer analysis; Heat flux

LIST OF PUBLICATIONS

International Journals

1. Development of innovative Rice Husk Ash based insulated mortar to enhance thermal performance in buildings– construction and building materials– Under review
2. Utilization of crushed tile coarse aggregate (CTCA) and rice husk ash (RHA) as partial replacements of natural coarse aggregate and binding material in concrete– Advances in Civil Engineering – Under review
3. Behaviour of CFRP strengthened concrete curved beam subject to out of plane bending -Engineering Structures– Under review

International Conferences

1. Thermal Performance of Rice Husk Ash mixed mortar in Concrete and Masonry Buildings - 10th International Conference on Advanced Models and New Concepts in Concrete and Masonry Structures, Poland, Lublin -Indexed conference- journal "Budownictwo i Architektura" (Civil Engineering and Architecture) https://doi.org/10.35784/bud-arch.2121
2. An investigation into the flexural behaviour of horizontally curved beams strengthened with NSM CFRP LAMINATES- International Conference on Civil Engineering and Application, Moratuwa, Sri Lanka - Published

Table of Contents

List of Figures

List of Tables

CHAPTER 1: INTRODUCTION

1.1 Background

The cement industry is contributing about 7% of global greenhouse gas emission (GHGE), and this contribution is significantly increasing every year as the demand of cement in construction industry continue to grow worldwide [1]. Sand is a major raw material used as filler to produce concrete, mortar, ceramics, glass, brick, tile and etc. [2]. About 40% of sand is consumed by the construction industry all over the world, which is about 10 billion ton per year [3]. This sand usage will increase significantly in 2030 as the population of building construction anticipated to hit 8.5 billion [4]. The over utilization of sand has serious environmental, economic and social impacts [5].

The major environmental impacts of sand mining are deforestation, loss of biodiversity, soil erosion and air pollution [2]. These ecological impacts resulting from cement production and excessive sand exploitation call for some viable cleaner production solution in construction industry as sustainability options. Therefore, supplementary cementitious materials such as fly ash [6–8], silica fume [9–11], bottom ash [12,13], blast furnace slag [14–16], metakaolin [17,18], biochar [1,10], waste glass [19,20] and rice husk ash [21–23] are used as a partial or fully replacement for the cement and/or sand in the construction material to reduce the GHGE and environmental impacts.

Rice husk is an agricultural waste generated in high quantities while processing rice. Though it has been used as a major source of biomass for fuel generation and an energy source for electricity generation in many countries especially in Sri Lanka [24]. Rice husks are usually dumped in the open area, thus leading to contamination of water and consumption of large land space, thereby impacting the environment negatively without any economic benefits [25]. The open-air burning process is the most common disposal process of rice husk and it is producing significant amount of rice husk ash (RHA) waste in remote areas, which contributes to the air pollution and air borne respiratory issues. This unproper disposal of RHA waste cannot be classified as a complete cleaner production. Hence, use of such waste materials to develop green building materials is a sustainable approach [26].

RHA as a partial replacement for cement in concrete or mortar has been used in many countries as it is highly reactive pozzolans [26–30]. When rice husk is incinerated, it produces 17–20% mass of RHA out of the initial mass, that is a lightweight and highly porous material with a density in the range of 180–200 kg/m3 [31,32]. The percentage of silica (SiO_2) in rice husk ash produced from controlled burnt condition is normally account from 85-90% [33,34]. This high percentage SiO_2 reacted with the hydrated product of cement and producing extra C-S-H gel and improve the strength of mortar or concrete [35]. Further, most of the previous research studies investigated the usage of proper treated RHA as a partial replacement of cement in concrete or mortar [39–41]. Moreover, the use of rice husk ash as building materials are limited to replacing rice husk ash as cementing material but not as a filler material/fine aggregate. Thus, this study focused on the effect of mechanical, thermal and environmental performance of mortar with RHA replacing the sand.

The combustion temperature of 600°C for 2 hours is the best combustion temperature to produce highly reactive RHA in controlled condition, which is white in color [37]. A study by Jamil et al. [39] found that the compressive strength of RHA mixed mortar significantly increases with the increase of RHA content and reported that about 20% replacement of cement with 6.72 µm particle size RHA is feasible. A study by Siddika et al. [40] found that 10% of cement replacement with RHA exerts the maximum gain on compressive, flexural and tensile properties in concrete. All these studies are focused on properly burnt and grounded rice husk ash, which is named as controlled burnt RHA (LRHA). The approach to produce the LRHA for durable concrete or mortar is an energy-intensive approach and contribute embodied GHGE.

The rice husk is also used as fuel for steam boilers to produce the rice in many countries [41]. This process resulted in the production of large amount of black RHA and named as open burnt RHA (HRHA). The HRHA called as high-carbon RHA which is black in color containing many unburnt carbon particles [11]. A study by Chatveera et al. [42] found the usage of black color RHA which is produced from a rice mill also have positive impact in producing concrete. The use of HRHA in mortar or concrete reduces the embodied energy and related GHGE than the LRHA. Hu et al. [25] pointed that the production stage of 1 kg LRHA released 0.157 kg CO_2-eq. Whilst, the CO_2 emission from HRHA considered to be zero as it does not contribute to global warming [31]. Thus, this study is aims to use RHA waste generated from rice mills to produce the sustainable mortar for wall plaster.

Wall plaster plays a very active role in the thermal performance and comfort of building. The mortar with high distribution of pores and low-density particles will improve the thermal performance as it reduces the thermal conductivity [1]. RHA have high potential to produce thermal insulation mortar due to their pores and light weight nature. Very limited information is available in the current literature on the thermal conductivity of cement plaster containing RHA. Hence use of rice husk ash waste materials for developing green materials could lead to economical and feasible applications while reducing the environmental impacts and energy usage. In addition, almost all RHA based mortar/plaster was focused only on the satisfaction of mechanical properties and no attention was made to keep the balance between the thermal and mechanical properties of the end product.

Epoxy adhesive is very likely to change temperatures in the building industry. The epoxy temperature is to preserve the stability of Carbon Fibre Reinforced Polymer (CFRP) and concrete at a high temperature and the glass transition temperature of the CFRP is 70 ^{o}C. Concrete composites hit the collapsing point within 5.5–6 minutes under normal fire contact. This suggests that the reinforced concrete members of CFRP need to provide a sound insulation system network [1]–[4].

Heat insulation mainly aims at protecting or shielding the fiber-enhanced polymer (CFRP) from high temperatures. Exposure to high temperatures without thermal insulation results in strength reduction and peeling of fiber-reinforced polymer repair material leads to a reduction of the load-bearing capacity of the retrofitted structural component as well as a loss of rigidity and stability [4], [5].

The main aim of the research is to develop an insulation plaster to use as a shield for CFRP under high temperatures. Currently, in the market, Vermitex is the product available for the insulation of CFRP and concrete system which is a very high cost. The main objective of the research is to develop a plaster for insulation to be used as a high-temperature CFRP shield. Vermitex is only available in the market at a high cost. That is the main objective of the analysis, which essentially generates an equivalent product using RHA waste.

1.2 Significance of research

Thermal performance of FRP/Concrete members retrofitted using other methods than Near surface mounted (NSM) and externally bonded reinforcement (EBR) has not been investigated. The waste products have not been much incorporated for developing insulation plaster for FRP/Concrete composites.

1.3 Aim and objectives

The aim of this research project is to develop an innovative rice husk based insulated plaster to enhance thermal performance in buildings while keeping the required strength cost effectively.

The specific objectives of this work:

1. To develop a cost-effective insulation plaster using RHA.
2. Investigate the heat transfer analysis of the insulation plaster.
3. Investigate the Life Cycle Assessment (LCA) of developed insulation plaster.
4. To study the thermo-mechanical behaviour of FRP/Concrete composites using developed insulation systems for FRP-concrete composites.
5. Evaluate the thermal performance of developed insulation plaster in CFRP/concrete composites.

1.4 The Arrangement of the Thesis

In this report, the research project has been presented with ten chapters.

CHAPTER 1: The first chapter contains the introduction, objectives, and methodology of the research.

CHAPTER 2: The detailed literature review which explains the background of this topic.

CHAPTER 3: The details of the methodology and testing methods with relevant codes.

CHAPTER 4: Low carbon RHA (LRHA) AND High carbon RHA (HRHA).

CHAPTER 5: Improvement of mechanical properties and economic analysis.

CHAPTER 6: Life cycle assessment (LCA) of RHA-based mortar.

CHAPTER 7: Heat transfer analysis.

CHAPTER 8: Testing related to CFRP and insulation plaster.

CHAPTER 9: The conclusions relevant to the research that have been done as well as recommendations.

1.5 Chapter Summary

This chapter clearly introduces the validations for using the rice husk ash in mortar as a partial substitution of sand which has been not studied in other research. It presents the main aim of the study as using this agricultural waste as an insulation plaster for CFRP/concrete composites and assesses the need for rice husk in industry. It also gives a brief outline of the other chapters.

CHAPTER 2: LITERATURE REVIEW

2.1 Introduction

In the last century, many countries have conducted research on using rice husk ash in concrete. RHA is an agricultural waste product, meaning a large amount of silica, with very good processability. Rice husks are the natural sheaths forming on rice grains during their growth; these are extracted during rice milling, although they do not appear to be of commercial value. It can however be made useful across several thermochemical conversion processes.

Mehta [6] was the first person to play a significant role in 1970 in using rice husk ash in concrete. The burning state defines mainly the effectiveness of rice husk ash whether the material is highly reactive. He is the person who constructs a good knowledge of the proper burning condition of rice husk ash until all uses are in the way of uncontrolled combustion. Many researchers investigated the burning condition after this key point and found many solutions for better methods of burning.

Many research works focused on reducing the cement content in concrete and thereby reduce the amount of CO_2 emission. Meryman et al. [7] identified that the usage of supplementary cementitious materials (SCM) in concrete as the partial replacement of cement helps to reduce the emissions of CO_2. They used many substitutional materials such as Fly ash, RHA, limestone, bottom ash, palm oil, and various materials to check the impact of strength, workability, and other durability properties while reducing the amount of cement usage.

Carbon Fiber Reinforced Polymer (CFRP) [8] is a commonly practicing retrofitting material for structural elements from the past few decades significantly. The main advantage of using CFRP is the very high strength to weight ratio compared to other structural materials. Also, the flexibility of raw CFRP sheets provides a great deal of easiness over applying the CFRP to the structural elements.

However, there is a need for an insulation system to protect the CFRP in case of fire because above the glass transition temperature profile the properties of CFRP getting deteriorated. To avoid such a situation there are many insulation products available in the market which are very expensive. So, the main intension of the literature review is to find out the low-cost sustainable insulation system using locally available material in Sri Lanka to avoid the failure of CFRP properties. The literature review below discusses contributions to this area, which are important to the reach of this study so far.

2.1.1 Building insulation materials

Around the world, the construction industry absorbs nearly one-third of operating energy of buildings, resulting in greenhouse gas emissions. The quantity of carbon emissions will result in a 53% rise in the next decade due to population growth and increased demand for lifestyles with new technologies, which will be a big challenge for our atmosphere. Insulation materials are used to balance the need for heating and cooling in buildings and help improve the buildings' thermal comfort. There are mainly 3 types of insulation building materials [9].

1. Conventional
2. State-of-the-art
3. Sustainable

Among them, sustainable building insulation materials have the lowest impact on the environment, which ensures that embodied energy for the stage of production and carbon emissions for sustainable building materials are minimal. Examples of certain sustainable insulation materials are shown in Figure 2.1. They are still in use as materials for construction insulation. So, on this line, rice husk is also a waste created in enormous quantities all over the world especially in Sri Lanka. This inspired me to choose rice husk waste to create an insulation material. There are primarily three things to concentrate on in order to pick an optimal building insulation material- parameters, indicators and criteria. The key parameters to consider in order to choose a good insulation material are thermal conductivity, heat capacity and embodied energy. Energy, environment and economic aspects need to be assessed as criteria when choosing a insulation material.

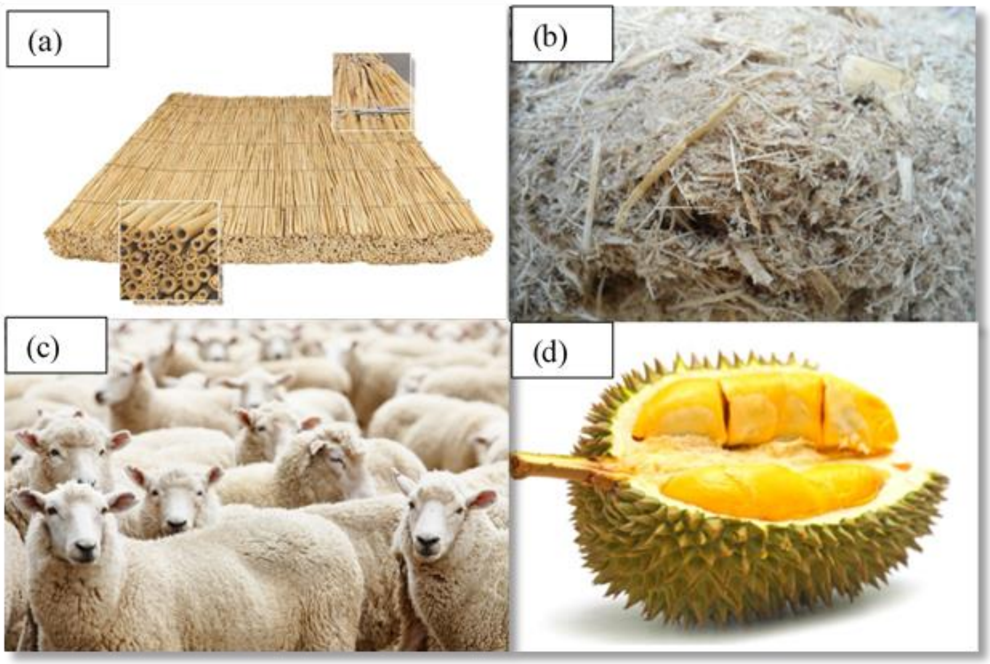

Figure 2.1: Sustainable building insulation materials a) Reed panel b) Sugar cane c) Sheep wool d) Durian plant

2.2 Rice husk

Nowadays, Rice has been the most important food in everyone's life in more than 100 countries where millions of people consume. During the last 15 years, paddy cultivation increased by almost around 50 % [10]. The annual production of rice is illustrated in Figure 2.2.

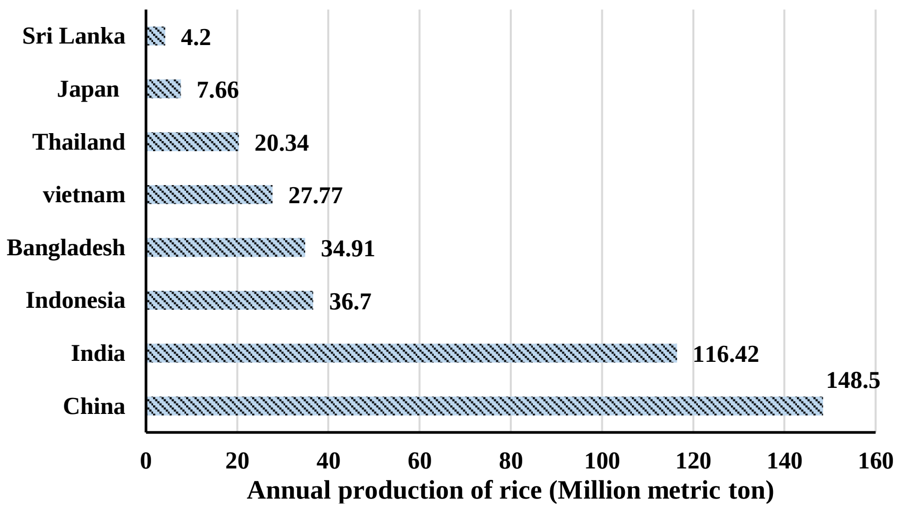

Figure 2.82: Annual production of rice around the world 2018/2019

In the period of 2018/2019, the paddy cultivation in all over the world was approximately 212.72 Million Hectares and rice production of about 425 million metric tons recorded from Asia (FAOSTAT, 2018/2019).

Agriculture has contributed approximately 7% to the GDP in Sri Lanka. Rice husk contributed as the primary energy source in some industries in industrial zones in the country. The areas in some districts such as Anuradhapura, Polonnaruwa, Kurunegala, and Jaffna which produce rice are consisting of the huge quantity of RHA that is accumulated after the usage of rice husk as a fuel (Figure 2.3).

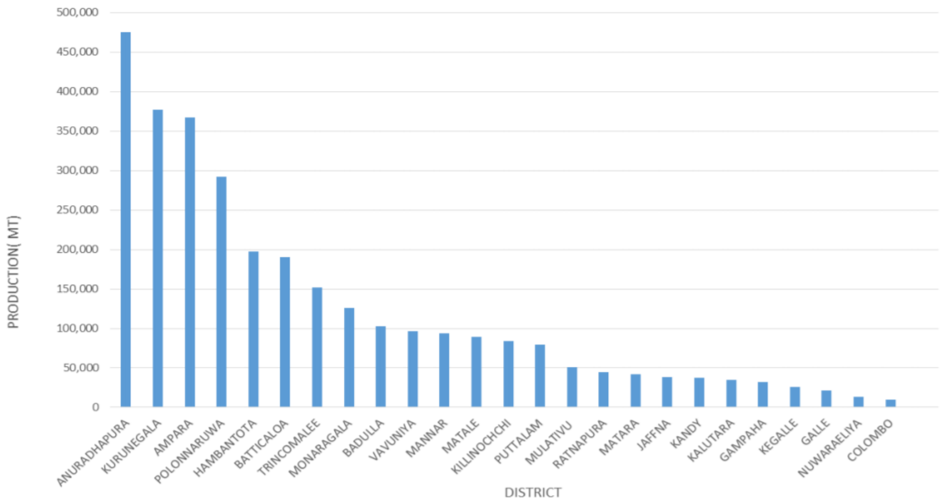

Figure 2.83: Annual production of rice in all the districts of Sri Lanka 2018/2019 MAHA SEASON

2.3 Characterizations of RHA

RHA is a common term that clearly depicts all the types of ash produced by the incineration of rice husk. Normally the incineration of rice husk produces 17% to 20% of very lightweight material rice husk ash which is highly porous with a density of approximately 180-200 kg/m^3. White rice husk ash, gray rice husk ash, and black rice husk ash are the three different types of RHA which are categorized by burning temperature and burning time. Above 700 ^{o}C of burning can produce white rice husk ash under controlled conditions [11], [12]. White rice husk ash has more silica content than other forms of RHA which shows a good pozzolanic property when compared to black rice husk ash. The uncontrolled form of burning condition (Black RHA) results in the formation of more carbon residuals which show low mechanical characteristics when compared to controlled burned samples (White RHA) [11].

The RHA microstructure known as SEM photographs is shown in Figure 2.4. The temperature of burning in the furnace is 600 °C constant for 2 hours. From the photographs, it has been observed that most components are retained after oven burning and only some components have become structurally degraded. Further, the internal surface (Figure 2.4B) and external surfaces (Figure 2.4A) are very dense clearly shows that the surfaces are covered with a very rough membrane without any pores [13].

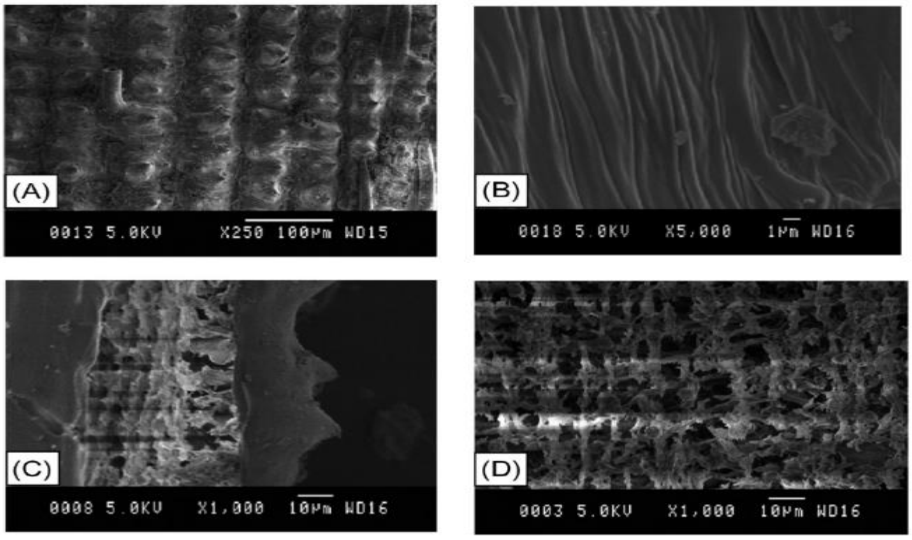

Figure 2.84: Microstructure of RHA (A) Outer Surface (B) Inner surface area (C) Side surface and (D) Intermediate layer

Cross-section of the rice husk ash from the SEM studies reveals that the outside surface of the rice husk ash is thicker than the internal side and there is an intermediate surface consists of a crisscross mesh of chips between the inner surface and outer surface. Figure 2.3(D) clearly shows that the chips contain more numbers of holes in the shape of honeycomb which are in the range of nanometers. These nano-sized pores are created by the SiO_2 particles depends on the burning condition too. The specific surface area and reactivity of RHA mainly depend on the amount of silica content [13].

2.4 Properties of RHA

Many factors that affect the SiO_2 content, carbon residual, appearance, and color of RHA. Mainly, they are burning temperature, burning duration, burning method, treatment of material, geographical location, and the usage of fertilizer. The chemical composition of RHA is SiO_2, K_2O, P_2O_5, CaO, Na_2O, and C. RHA contains higher amount of silica which may range from 85 % to 95 % [14]–[16].

The contents of K_2O and Na_2O reflect the fertilizer levels used and the type of soil used during paddy growth. Temperature plays a crucial role in affecting RHA's pozzolanic nature. A lot of researchers have been studied the type of furnace used to obtain the standard RHA form. Of those processes, the most effective approach for generating good RHA is the use of the fluidized bed cycle [17].

Fernandes et al. [18] investigated the chemical composition, surface area, LOI, and various types of burning methods. From his research, it was concluded that the combustion method influences the amount of SiO_2, loss of ignition point, and surface area of RHA.

2.5 Applications of RHA in concrete

In the later part of the 2000s, usage of RHA as supplementary cementitious material in concrete has undergone huge improvements. Many researchers investigated the usage of RHA and proved that it can improve the mechanical properties especially the strength parameter and helps to minimize the shrinkage. The major problem of using the RHA in concrete is the water absorptions. It absorbs more water than the control mix. Usage of RHA up to 10 % can help to improve the compressive strength. RHA concrete has a high resistance to corrosion of acid when compared to concrete without RHA. RHA can be used as a marine concrete because of its nature which can improve the chloride resistance. RHA is used to produce concrete blocks with the usage of allowable limits [7], [19].

2.6 Physical properties of RHA

RHA is very tiny particle sizes in the range of 6-10 μm and usually below 45 μm. Figure 2.5 shows Scanning electron microscope (SEM) images of RHA with a very cellular porous nature with a small area which is three times larger than silica fumes in the 0.1 to 1 μm range. Grinding the RHA to high fineness does not affect the mechanical properties, as the surface area is the main factor affecting the pozzolanic property and grinding of RHA also helps to minimize water absorption. Because of RHA's high porosity, it displays a low water absorption rate that affects fresh concrete properties [20], [21].

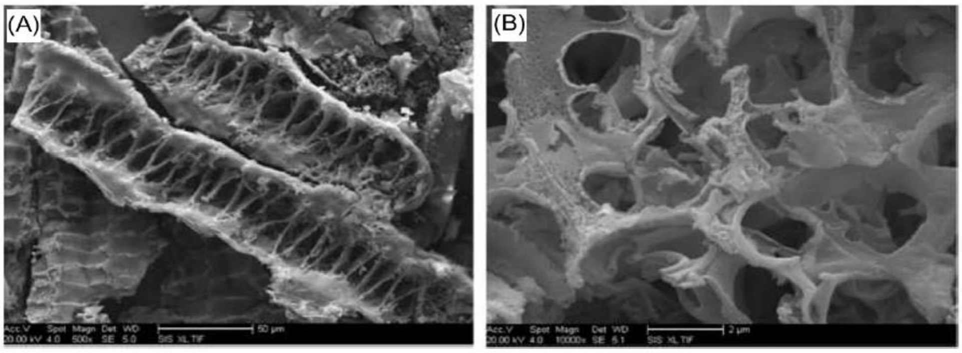

Figure 2.85: SEM photographs of RHA (A) 500 × (B) 1000 × magnification level

Figure 2.6 shows the raw material rice husk, burnt rice husk ash, and the RHA after grinding which clearly shows the particle size variations. The important physical properties of RHA studies by the various researches are given in Table 2.1 [22], [23].

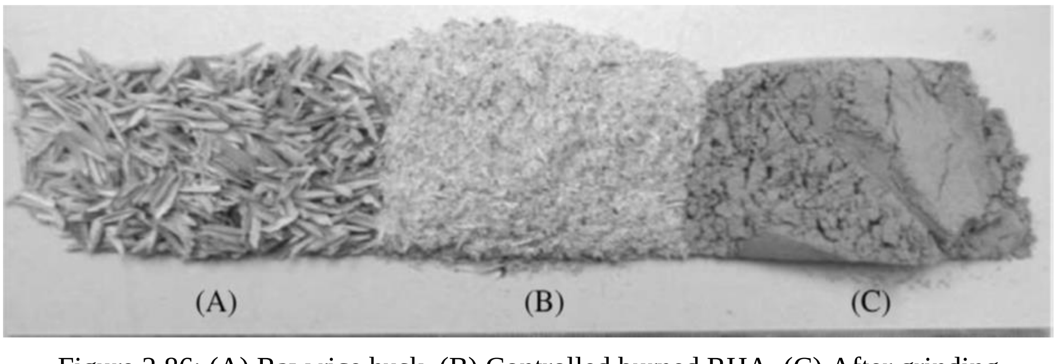

Figure 2.86: (A) Raw rice husk, (B) Controlled burned RHA, (C) After grinding

Table 2.1: Physical properties of RHA [24]–[27]

	Mehta (1992)	Bui et al. (2005)	Ganesan et al. (2008)	Zhang and Malhotra (1996)	Feng et al. (2004)
Mean particle size (μm)		5	3.80		7.4
Specific gravity	2.06	2.10	2.06	2.06	2.10
Fineness	99		99	99	
Specific surface (m^2/g)			36.47		

2.7 Particle size distribution

From the studies of Della et al. burning the RHA for 6 hours at 700 ^{o}C, results in the particle size of around 33 μm on average [28], [29]. After grinding the samples for more than one hour, the average particle size was reduced to 0.68 μm. From his studies, it can be concluded that the particle sizes are important in the mechanical properties of RHA concrete when compared to other research studies. Figure 2.7 presents the particle size distribution of sample RHA from a rice mill obtained by Agarwal [30].

The specific surface of improperly burned rice husk particles is more than the controlled burnt samples. Della et al. [25] found that the variation of this parameter is proportional to the burning temperature and the time of the burning. Table 2.2 shows the variation of specific surface areas with different conditions.

Table 2.2: Specific surface area of RHA in different condition [28]

Improperly burnt	Controlled burnt	After grinding
177 m^2/g	54 m^2/g	81 m^2/g

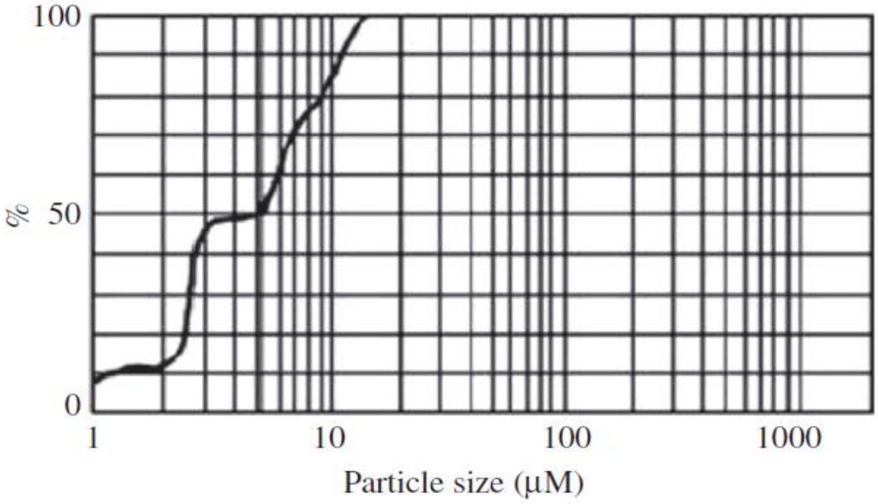

Figure 2.87: Variation of particle size of RHA

2.8 Mechanical properties of RHA

2.8.1 Flowability

The replacement of RHA with concrete reduces the initial slump as more water is absorbed. Therefore, the high water-cement ratio is recommended to achieve the proper slump or to add the mixture to make the required flow level.

Adding RHA to cement substitution by less than 3 percent would be effective in enhancing concrete workability at a given water-cement ratio. Ikpong and Okpala noticed slump variation with different RHA replacement level by replacing cement at 30 percent and 40 percent for various mix designs. Their results are presented in Table 2.3. It can be concluded from the table that RHA concrete requires more water content to achieve the required slump compared with concrete without RHA [31], [32].

Table 2.3: Variation of slump with different replacement levels of RHA [33]

Compressive strength (MPa)	RHA (%)	W/C ratio	Slump (mm)
20	0	0.80	40
	30	0.83	33
	40	0.85	35
25	0	0.69	35
	30	0.72	35
	40	0.75	37
30	0	0.64	50
	30	0.64	55
	40	0.65	35
40	0	0.54	50
	30	0.57	45
	40	0.61	45

2.8.2 Compressive strength

The application of pozzolanic materials to concrete would impact primarily the compressive strength and permeability of the mechanical properties. Because of its porous nature, RHA absorbs more water resulting in bleeding reduction and helps to avoid water saturation with the aggregates. Figure 2.8 shows the variation of compressive strength with RHA replacement levels for two different types of RHA which are grounded and ungrounded particles from the studies of Chandra et al. [34]. He found that if the replacement levels go beyond 5 %, compressive strength goes down than control mix.

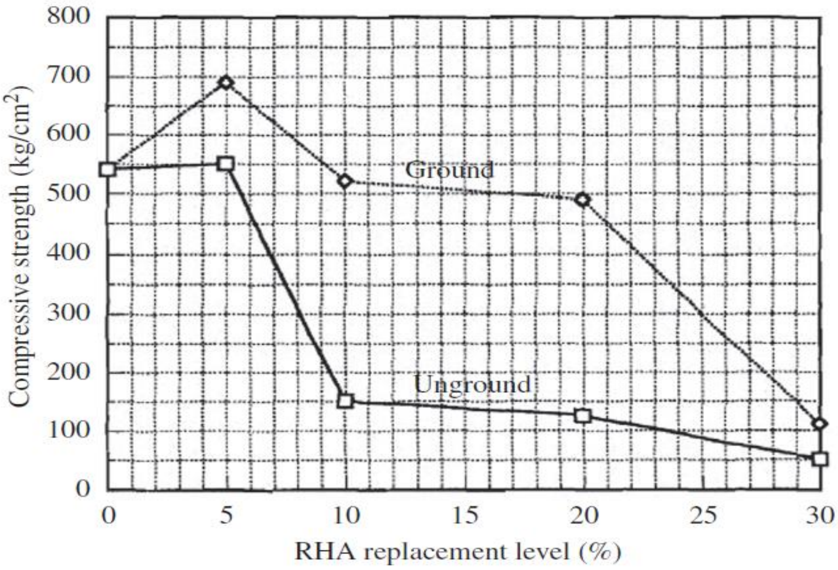

Figure 2.88: Compressive strength variation with RHA replacement levels [34]

The early-stage strength of the concrete is mainly depending on w/c ratio. As the addition of pozzolanic material results in the reduction of workability, it affects the early strength of the concrete. Table 2.4 illustrates the variation of compressive strength with the development of ages clearly shows that the increment of strength is more in 90 days of curing. Most of the mixes achieved more than 60% of strength in 28 days [14].

Sensale et al. [35] examined the two different forms of rice husk ash with one ash from Uruguay (39.55% silica) and others from the USA (98.5% silica). He found that the concrete contains USA ash had higher compressive strength than Uruguay. At 90 days, concrete comprising RHA shows more strength development than control concrete. A 20 % replacement level is the optimum level to achieve adequate strength. When comparing both types of concrete, Uruguay RHA concrete is not as strong as the USA in the long term.

Table 2.4: Variation of compressive strength for different mix design with the development of ages [36]

Mix design	RHA (%)	Compressive strength (N/mm^2)			
		7 days	14 days	28 days	90 days
20	0	17.5	23.9	33.1	37.8
	30	15.8	18.2	29.1	36.1
	40	3.27	15.2	27.2	33.9
25	0	22.9	27.2	35.4	39.2
	30	18.7	23.8	31.1	37.5
	40	14.8	21.0	28.6	34.0
30	0	28.4	37.6	43.5	46.3
	30	22.6	32.0	38.3	43.2
	40	16.7	27.5	31.8	37.1
40	0	32.4	38.8	44.2	47.6
	30	24.0	33.5	39.4	44.9
	40	1.5	29.3	34.6	38.9

2.8.3 Water absorption

Mayooran et.al 's [11] findings have shown that the effects of water movement within the cement block are the principal agents for material deterioration. The main reasons for this behaviour are the freeze-thaw damage, and the water can lead to the transport of chloride ions, sulfates ions, and other ions. Therefore, it has a significant effect on the toughness of the cement block absorption. The water absorption from the RHA cement blocks was higher than the conventional cement block, as expected. The porous nature of the RHA particles is the main reason.

Using RHA with lime mortar helps to reduce the water demand of hydrated mortar with the required w/c ratio. Ganesan et al. [37] found that the replacement of RHA in mortar increases the water demand but it has lower demand than hydrated lime mortar.

2.8.4 Bulk Density

Bulk density is the parameter inversely related to the absorption of water. Most of the RHA blocks show significantly lower bulk density than blocks without RHA with the range of 1600 – 1800 kg/m^3 which stratify the minimum requirement of the bulk density. Dry density shows a huge reduction when compared to control blocks as it absorbs more water than concrete without RHA [15].

The reason for the reduction of bulk density is mainly due to the lower specific gravity of RHA particles replaced by the higher density fine aggregates which help to reduce the weight of samples and caused the lower value of density. When the replacement level goes more, the weight of concrete blocks results in very lightweight material when compared to a normal concrete block. The bulk density of the sample with a 10 % replacement level is 1893 kg/m^3 [38].

2.9 Thermal insulation materials

Several types of thermal insulation materials are available for the construction industry as shown in Table 2.5.

Table 2.5: Thermal conductivity value of insulation material mixed with cement mortar

Insulation material	Thermal conductivity (W/m K)	Ref.
Bottom Ash	0.523	[39]
Blast furnace slag (BFS)	1.017	[40]
Rubber waste	0.598	[41]
Ferronickel Slag	1.16	[42]
Wood waste	0.62	[43]

Fly ash	0.792	[44]
Banana fibre	0.523	[45]
Date palm	0.14	[46]
Expanded polystyrene (EPS)	0.034	[47]

Ghosh et al. [44] also studied the reuse of fly ash in mortars to increase the buildings' thermal efficiency. Two types of mortars were used with 1:6 and 1:4 cement: sand and sand were replaced with a 10 percent to 100 percent higher percentage of fly ash (Ghosh et al. 2018). For both grades, it has been found that the thermal conductivity of mortar would improve with the increasing amount of fly ash. The compressive strength however decreases with increasing removal of fly ash.

Ghost et al. [44] researched the reuse of bottom ash in cement mortar for buildings with improved thermal efficiency. The increase in bottom ash has been shown to also reduce the thermal conductivity and compressive strength (Ghosh et al., 2018). The thermal performance in the bottom ash mixed mortar was higher as compared with fly ash and bottom ash and the mechanical properties were lower in fly ash mixed mortar. It was discovered that fly ash and bottom ash replacing the river sand would decrease thermal conductivity to 0.29 and 0.28, respectively. It has been attributed to the decreased porosity of cement mortar blended with bottom ash.

2.10 Insulation plaster for CFRP/Concrete composites

Calcium silicate surface system, dense coating system, and Ultrathin coating system thermal conductivities are 0.06, 0.12, and 0.06, respectively. For CFRP bonded reinforced concrete beams with calcium silicate surface insulation, dense coating, and ultrathin fire proof coating over the entire duration, sufficient fire resistance of 2 hours has been obtained [1]. Vermitex-TX has been used as a fire safety insulation agent and has a thermal conductivity of 0.127 W / m K and is widely available on the market.

The Perlite mortar and Vermiculate mortar thermal conductivity values are 0.28, and 0.32, respectively. Perlite mortar displayed 2.5 times lower thermal conductivity relative to Vermiculate mortar and had a compressive strength limit. No capacity loss was observed when filled at 500 °C for 3 hours and cooled, then charged to failure, in the beams covered with a thermal insulation sheet [48]. In fact, steel wire mesh was inserted in the sheet of insulation and was able to shield the coating from splitting and eroding under heat. The use of this approach in the reinforced concrete slabs and columns was also proposed. But it was specified that the correct thickness of the coating should be used according to the specifications of fire safety.

2.11 Research gap

While considering past research papers about the usage of RHA in mortar and concrete, they have researched on rice husk ash as a partial replacement for cement in mortar and concrete. All have used LRHA for their study. Still HRHA (open-air burnt) is not used as a partial replacement for sand in mortar. As well as past researchers investigated the mechanical and physical properties of RHA replaced mortar. But thermal characteristics of HRHA and LRHA replacements are not focused on their studies so far. So, the main goal of the research is to investigate the material property, thermal property, and mechanical properties of RHA replaced mortar.

CHAPTER 3: METHODOLOGY

Laboratory Tests were performed under three stages (Tests for raw materials, Tests for fresh mortar, and Tests for hardened mortar) as shown in Figure 3.1.

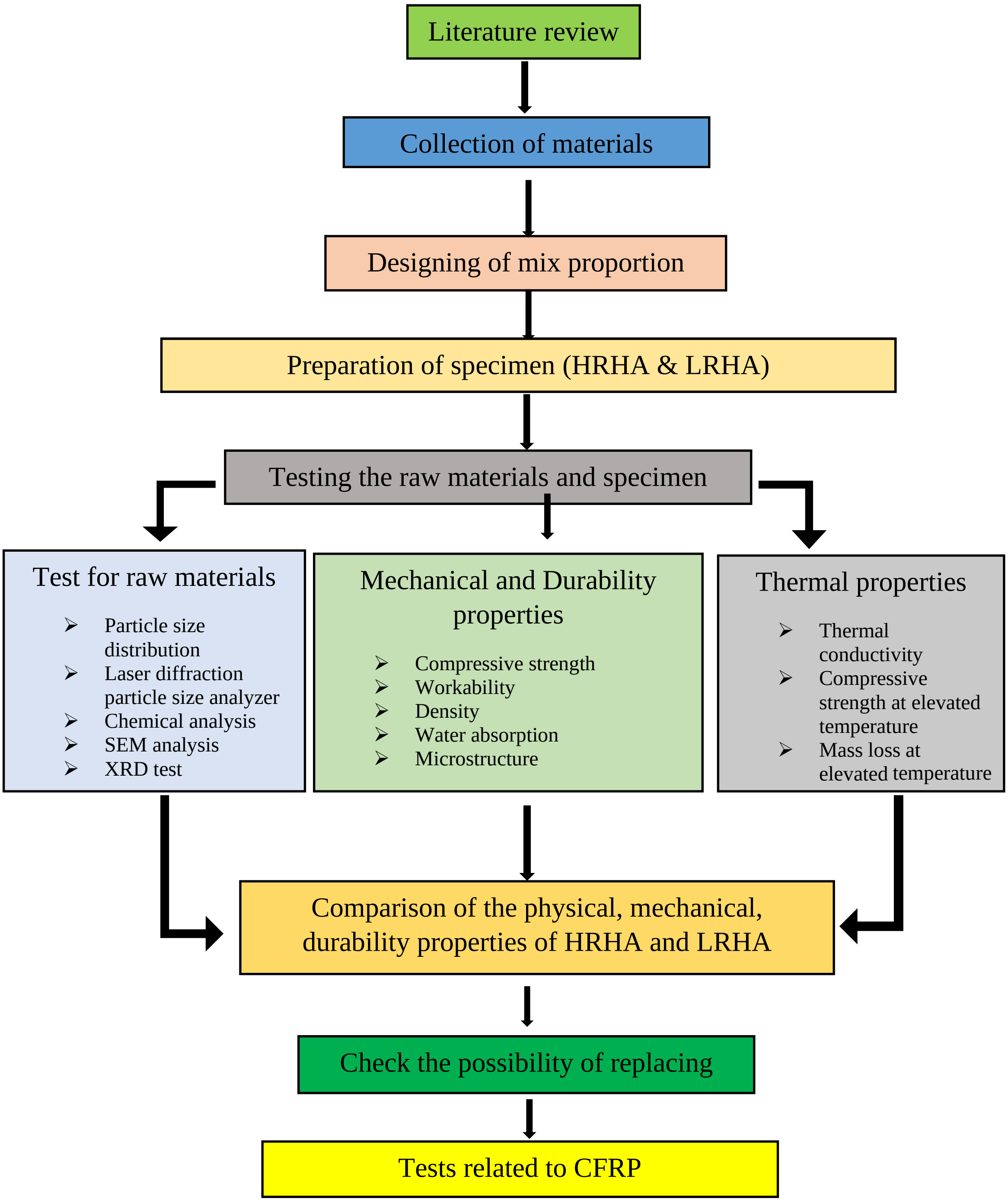

Figure 3.1: Experimental layout

3.1 Raw materials

Portland Limestone Cement (INSEE Cement), RHA, sand, and water were used as raw materials (Figure 3.2 and Figure 3.3) for the manufacturing of the waste substituted mortar cubes.

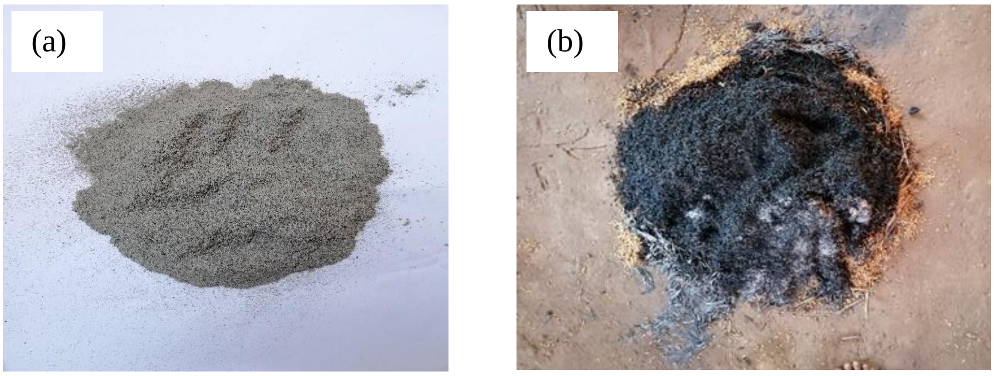

Figure 3.2: a) Low carbon Rice Husk Ash b) High carbon Rice Husk Ash

Figure 3.3: Different types of RHA

3.1.1 Materials used in samples

The following materials were used in the preparation of mortar samples to investigate the material and thermal characteristics according to the standard testing procedures.

- Cement: Portland Cement (A Portland Limestone cement under BS EN 197-1:2011 standard and complying with SLS 1253:2015)
- Sand: well-graded river sand with the size range of 0.25-1.18 mm was used in all the mortar mixtures
- Low carbon Rice Husk Ash (RHA): Obtained from a factory in Hiripitiya, geographically located in Kurunegala district in Sri Lanka where RHA is producing at high temperature (600 °C) in controlled burning conditions.
- High carbon Rice Husk Ash (RHA): Rice Husk was burnt outdoors for about 60 min under uncontrolled condition. This method is expected to yield more than 70 percent amorphous silica. The produced RHA was then received after proper incineration.

3.2 Laboratory test for raw materials

3.2.1 Particle Size Distribution

Knowledge regarding particle size, shape, porosity, and pore distribution of constituent materials is very useful to choose from and to use them in construction. Analysis of materials of different grain sizes, form, a composition by method of laser diffraction has been documented in this thesis to determine their suitability and efficiency for particular materials. The study revealed that mechanical sieving is efficient for granular materials ranging from 45 μm to 125 mm in thickness, but this approach provides insufficient results when implemented for very fine particle agglomeration susceptible materials. On the other hand, the laser analysis is deemed satisfactory for PSD analysis of materials with a medium to coarse size classification, providing more concrete details on the actual structure, distribution, and volume of the particle of the substance.

3.2.1.1 Sieve Analysis Test

Sieve analysis is the most common method for measuring particle size distribution in granular materials. This testing method used to identify the various sizes of particles to compare with other material sizes. The sieve analysis test was carried out to define the particle size distribution in the sand. The sieve analysis was rendered using the 5 mm, 4.75 mm, 2.36 mm, 1.18 mm, 600 μm, 300 μm and 150, μm series of mesh sizes. In all mortar mixtures, sand particles in the size range of 0.25-1.18 mm have been used. Figure 3.4 shows the testing setup of sieve analysis.

Figure 3.4: Sieve analysis test

3.2.1.2 Laser Analysis Test

In laser diffraction, a detector calculates the particle size from the set of light intensity data. Porosity is a measure of the voids within a material's particles or grains. The distribution of porosity and pore size is a function of porous geometry that is directly influenced by packing mass, particle size, particle form, and cementation. The instrument used to track the distribution of particle size of RHA as shown in Figure 3.5.

Figure 3.5: Laser Particle Analyzer

3.2.2 The microstructure of RHA

Pure RHA and Mortar containing various proportions of RHA were observed by Scanning Electron Microscope (SEM) –Model “Zeiss EVO 18”, to identify their particle size, distribution, and porous nature.

3.2.2.1 Collection of samples

First, small pieces of the mortar samples were cleaned well using high-pressure air, and then samples were arranged in an appropriate mould as shown in Figure 3.6. From the monitor, it was possible to observe the microstructure of mortar in every direction with different magnification levels.

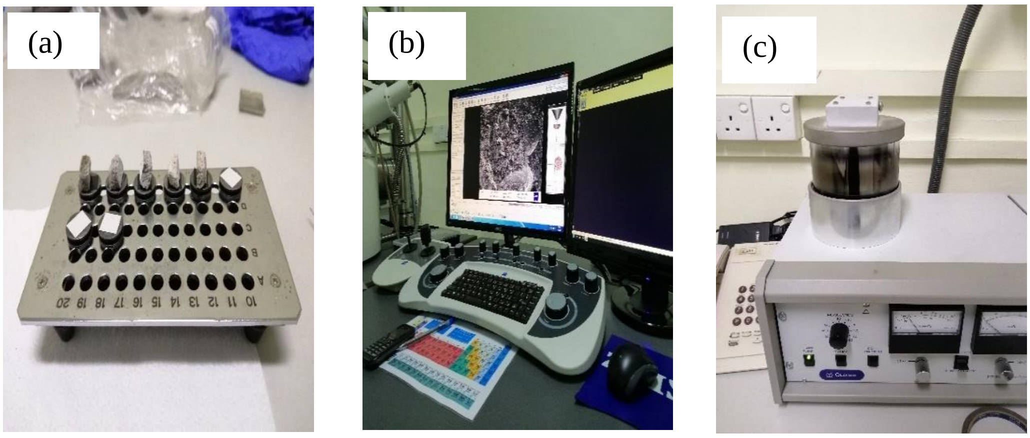

Figure 3.6: a) Sample preparation (b) Testing instrument (c) Cleaning the samples before testing under high pressure

3.3 Mortar sample preparation

The mortar mixes were formulated using a 1:3 ratio of cement, sand mass. Mortar specimens of RHA were prepared using different levels of replacement ratio. The water-cement ratio used for the control is 0.5. Depending on the past studies [2], the used ratios were determined by some practical guidance and several trial mixes. Rice husk was used as the sand replacement at different levels from 0-100 % of weight in mortar mixtures. Cement, sand, and RHA were blended correctly before the mixture is homogeneous. The combination contains warmth. Each blend was blended correctly. After that, it was poured into the mold and at a constant rate, the mixture was compacted by hand. The mold is discarded after half an hour and cast cement blocks were placed in an open atmosphere for hydration purposes. RHA replacement ratio also increased cement mixer stiffness and decreased workability. So, it was required to add more water to the mix. Table 3.1 shows the details of the number of samples used for the testing.

Table 3.1: Required specimens for test

Testing	**Control mortar**		**High carbon RHA (10, 20, 30, 50, 70, 80, 100)**		**Low carbon RHA (10, 20, 30, 50, 70, 80, 100)**	
	70 * 70 * 70 mm Specimens	**Specimens for thermal conductivity**	**70 * 70 * 70 mm Specimens**	**Specimens for thermal conductivity**	**70 * 70 * 70 mm Specimens**	**Specimens for thermal conductivity**
Density	3		21		21	
Compressive strength (7 and 28 days)	6		42		42	

Thermal conductivity (28days)		2		14		14
Water absorption (28days)	3		21		21	
Thermal analysis (28 days)	3		21		21	
Total	15	2	105	14	105	14

ASTM C1437 [49] was used as the reference for the flowability of mortar. The control mixture without RHA had a flow diameter of 140 mm. The workability of the mortar mixture has been to decreased due to RHA inclusion, as the sand substitutes of the same RHA weight increase the basic surface area of the particles and boost water quality to preserve the homogeneity of the mixture. Therefore, changing w/c was used to preserve the homogeneity of the mixture to ensure a steady flow (140 mm). Table 3.2 summarizes the mixture of materials and the amount of water needed to achieve this Flow value equal to 140 mm. A Mortar mixer was used to properly blend the sample.

Table 3.2: Mix proportion of mortars containing different RHA replacement.

Mix	**Sand replacement**	**Cement (kg)**	**Sand (kg)**	**RHA (kg)**	**Water (kg)**
MX1	0	1.0	3.0	0.0	0.5
MX2	10%	1.0	2.7	0.3	0.78

MX3	20%	1.0	2.4	0.6	0.92
MX4	30%	1.0	2.1	0.9	1.24
MX5	50%	1.0	1.5	1.5	1.96
MX6	70%	1.0	0.9	2.1	2.24
MX7	80%	1.0	0.6	2.4	2.68
MX8	100%	1.0	0	3.0	3.06

Figure 3.7: (a) Prepared samples (b) Mechanical mixer

These mixes were classified into three groups.

Group I: Used to check the effect of adjusting the Low carbon RHA ratio on the property examined.

Group II: The effect of High Carbon RHA ratio variation on the characteristics examined is investigated.

Group III: This category is called to determine the impact of admixture on the selected blend with RHA on the characteristics evaluated.

3.3.1 Mixing, Casting and Curing

Specimens of mortar mixes with and without RHA were prepared using ordinary Portland cement. Using a mixer, these were combined before homogeneity is achieved. Then, water was added and mixed as shown in Table 3.2.

About the casting process, steel molds (70 mm in size) were used for casting and compacting the mortar samples using a vibration. The residual mortar was extracted from the surface of the specimen and removed using a trowel. Such molds were used to assess compressive strength, density, and absorption of water.

Samples were covered with plastic sheets after casting and put in a position at a temperature of 20±2 ^{o}C for 24 hours before remolding was done. For different ages (between 7 and 28 days), specimens were then treated by keeping in water tanks before testing time. The water in the tank was changed every two or three weeks.

3.4 Laboratory test for mortar

3.4.1 Workability test / Flow Test

Mortar mixtures were prepared according to ASTM C109 [50]. Figure 3.8 demonstrates the consistency of the mortar flow test. With this test, a truncated cone was filled to the center of the flow table with mortar samples and place. The truncated cone was removed leaving the sample of the mortar which was continuously dropped 25 times. The normal mix stipulates a flow scale from 130 mm to 140 mm.

Figure 3.8: Flow of the mix

3.4.2 Compressive strength test (Cube test)

Mixture preparation is done by mixing the cement, sand, and RHA materials to homogenize the mixture. Then, water was added to the mixture and mixed using a mixture running at an angular velocity of 50 rpm for 10 min. In compliance with ASTM C109 [50], the compressive strength test of mortar specimens with the dimension of 70 mm × 70 mm × 70 mm containing RHA was conducted as shown in Figure 3.9 after 7 days and 28 days of curing. The reported results are the average of three-sample.

Figure 3.9: Test for compressive strength

3.4.3 Water absorption test by immersion

Samples were put in the oven for 24 hours at a temperature of 105 °C after 28 days of curing. After 2 hours of drying in the oven, weight of the dry specimens have been measured. Then, at room temperature, the specimens were immersed for 24 hours in the water. After the removal of samples from water, the surface was washed by a towel and the weight of the specimens was measured. The water absorption of the specimens was measured according to Eq 3.1.

Water absorption = $(W_w - W_d)/W_d$ ------------------- Eq 3.1

Where W_w is the wet weight, W_d is the dry weight.

3.4.4 Bulk density

Bulk density of mortar cube was calculated by measuring the weight of the wet state hardened cube sample where the volume was known. Here, the cubes with 70 mm × 70 mm × 70 mm were used to measure the required dimension, and three samples in each replacement level of RHA were used to measure the bulk density using the Eq 3.2.

The test is performed after 28 days from the casting of the cement block.

- The initial weight of the block (W_i) was measured.
- Length (L_i), height (Hi), and width (B_i) of the cube were measured.
- Density (Di) of the cube was determined from Eq 3.2.

$$D_i = \frac{W_i(kg)}{L_i \times H_i \times B_i(m^3)} \quad \text{------------------- Eq 3.2}$$

3.4.5 Thermal conductivity

The specimens were prepared in circular shaped moulds with a 3 cm radius and 5 mm depth as shown in Figure 3.10 (a). All the specimens were tested after curing in water for 28 days. Thermal conductivity tests were performed using a device that is based on the principle of the Lee Disc method as shown in Figure 3.10 and Figure 3.11. The recorded values are from the three-sample average. This approach has two stages: i) the first is to put the sample in the center of two copper metal disks, turn on the heater and wait until the device reaches the steady-state, admit the heat flow from the sample to disk 1 is equal to the airflow from disk 1 known as heating stage ii) the second stage is to remove the disk 1 and place it in an appropriate position to enter the room temperature as shown in Figure 3.12. The samples were tested after 28 days of curing in water (Figure 3.10 b). The calculation of thermal conductivity was carried out by equalizing the equations of heat flux in the two stages [25]. Two samples were tested to get the average.

The Thermal conductivity of the samples was calculated using Eq 3.3.

$$\boldsymbol{mc\,\frac{dT}{dt} = kA\,\frac{(T2-T1)}{x}} \quad \text{-------------------Eq 3.3}$$

Where; k - Thermal conductivity of samples [W/m K], A – Area measured through the cross section [m^2] , x - Sample thickness [m] , (T2-T1) - Temperature difference [K] , m - Mass of the disk 1 [m] , c - Specific heat capacity disk 1 [J/kg K], dT/dt - Tangent slope of the cooling curve in T2 [K/s].

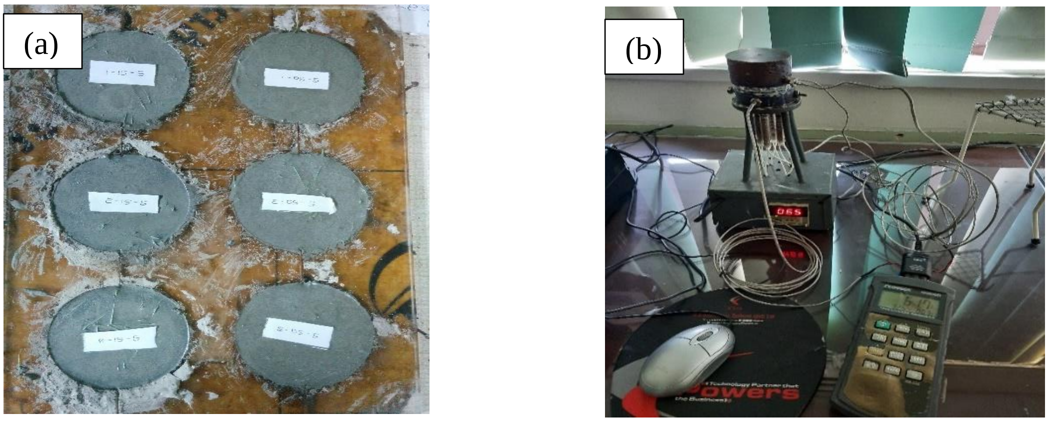

Figure 3.10: (a) Specimens to check thermal conductivity (b) Instrument used to check thermal conductivity

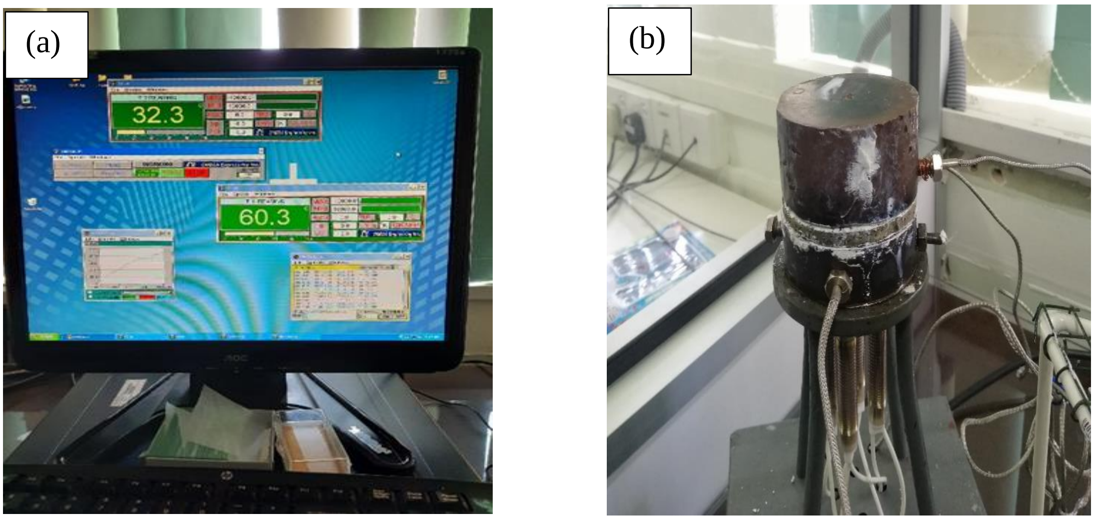

Figure 3.11: (a) Thermal conductivity instrument (b) Computer software for Lee’s apparatus

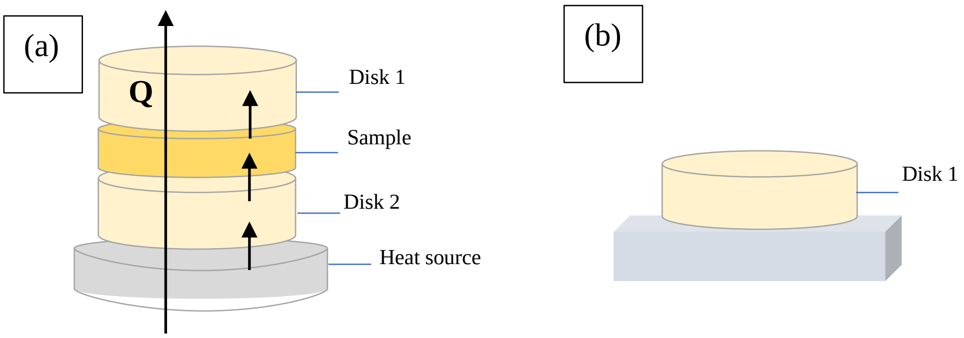

Figure 3.12: Schematic diagram of Lee's disk method: a) stage 1 b) stage 2

CHAPTER 4: LOW CARBON RHA (LRHA) AND HIGH CARBON RHA (HRHA)

4.1 Overview

RHA used in this analysis was collected from a factory in Hiripitiya, geographically located in the district of Kurunegala, in a controlled manner burning technique at about 600 ^{o}C for 2 hours which is physically grey in color. RHA grinding was done using an appropriate method.

The Particle size distribution curve of LRHA is presented in Figure 4.1. All the particles were passing through 350 µm and range from 0.15 µm to 350 µm.

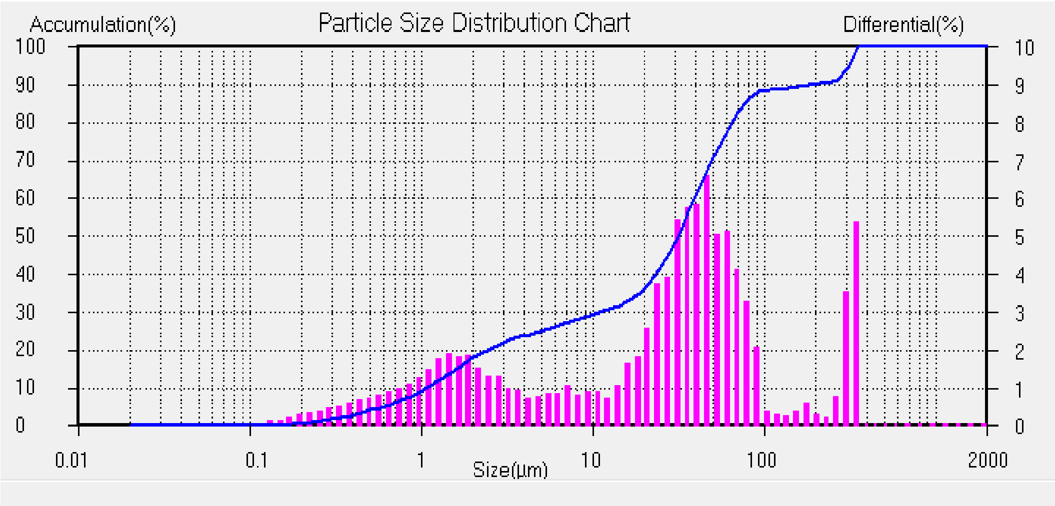

Figure 4.1: Particle size distribution of LRHA

From the figure, we can conclude that particles are very finer than fine aggregates. Table 4.1 shows the comparison of some particle's properties of cement, LRHA, and fine aggregates. Cement, LRHA, and natural sand average particle sizes are 11.96 µm, 21.37 µm, and 0.86 mm, respectively. Compared to cement average particle size, the used LRHA particles are large.

Table 4.1: Raw material properties

Type of sample	Specific gravity	Average particle size d_{50}	Specific surface area (m^2/cm^3)
Cement	3.12	11.96 µm	0.725
LRHA	**2.06**	**21.37 µm**	**1.191**
Sand	2.62	0.86 mm	-

4.2 Chemical composition

Table 4.2 shows the LRHA particles have a higher silica content of 81.4 % and the addition of SiO_2, Al_2O_3, Fe_2O_3 percent is greater than 70%, which is known as **F type** pozzolans in accordance with ASTM C618 [51]. Such claims relating to RHA's chemical properties are consistent with the findings previously reported [7] – [10].

Table 4.2: Comparison of chemical components

Materials	Wt %								
	SiO_2	Al_2O_3	Fe_2O_3	CaO	MgO	Na_2O	K_2O	SO_3	LOI
Cement	19.03	4.21	3.16	66.06	2.54	-	0.34	2.74	2.11
LRHA	**81.4**	**1.10**	**0.70**	**2.60**	**1.10**	**0.30**	**0.60**	**0.96**	**5.80**
Sand	93.42	2.41	1.51	0.41	0.10	0.10	0.90	-	0.68

4.3 Properties of LRHA incorporated mortar samples (Preliminary study)

4.3.1 Workability

Mortar workability was assessed based on the measured mortar flow. Flow is a direct indicator of a mortar's workability. Results indicate a decline of flowability when the replacement level of LRHA increases. This has happened probably due to high specific area and particle nature of the RHA which causes greater water demand. The mixture flow without LRHA was 140 mm, while mixture flow was 105 mm with 20%

of LRHA being replaced by sand. If the LRHA levels have gone above 30 percent, there is no flow which means that the water required is not enough to make the required flow as shown in Figure 4.2. Prior studies identified similar patterns [52]. So, it can be concluded that more water is needed to achieve the proper flowability of the mixture with LRHA. The increased demand for water can be due to the porous and spongy nature of LRHA which could contribute to an increase in LRHA surface area [11].

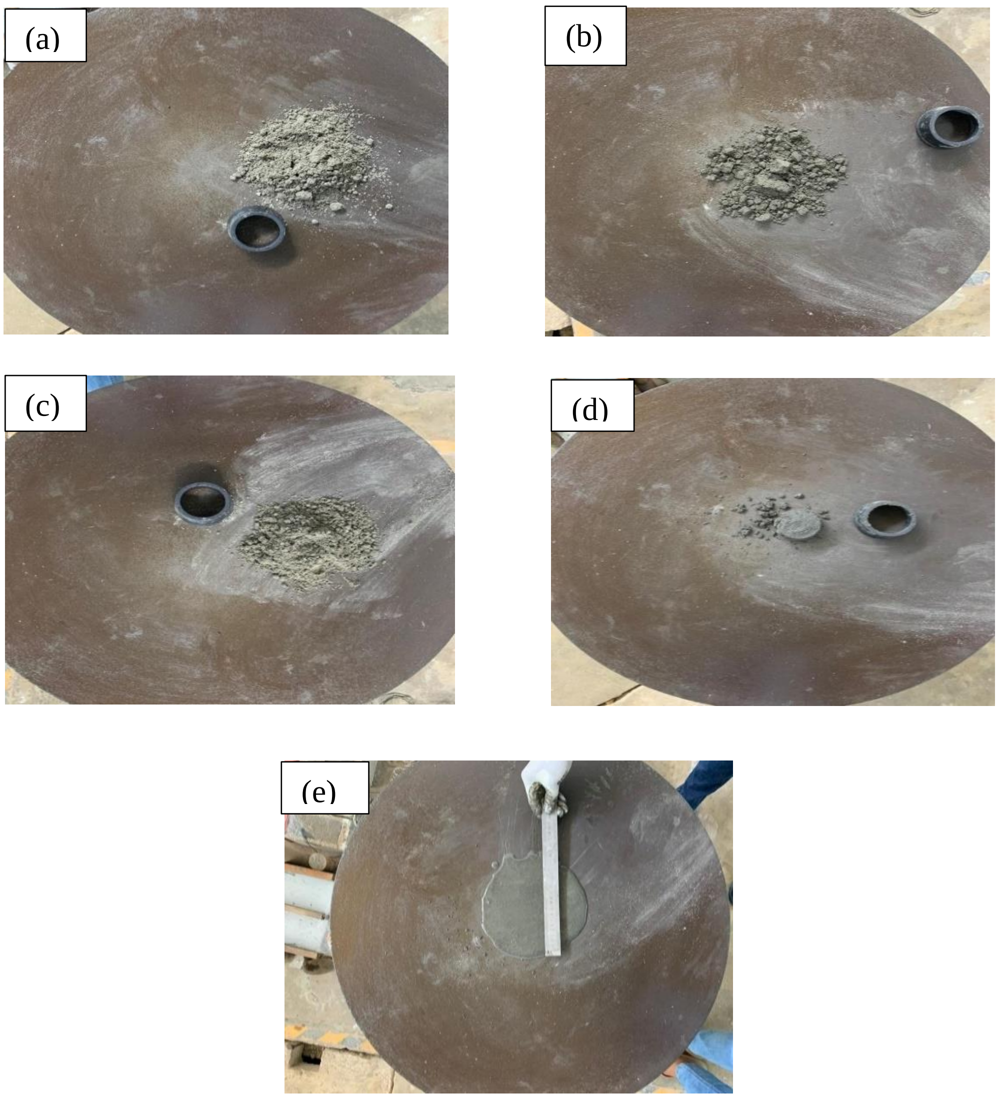

Figure 4.2: Variation of flow for different w/c ratio of 30 % replacement LRHA mix (a) 0.5; (b) 0.7; (c) 0.9; (d) 1.0; (e) 1.2

4.3.2 Compressive Strength

The compressive strength of mortar decreases drastically with the increase of LRHA particles as shown in Figure 4.3. The mortar containing up to 30 % LRHA shows a considerable compressive strength. Meanwhile, the replacement of sand with LRHA above 30 % shows a heavy reduction of the compressive strength. The limit of type N mortar which is used for general purpose should contain the minimum compressive strength of 5.2 MPa at 28 days according to ASTM C270 [11]. The average compressive strength of specimen with 50 % RHA replacement is 4.8 MPa and it is less than the minimum requirement. This behaviour is due to the addition of low-density LRHA which leads to an increase in porosity of developed mortar. A similar trend was observed in previous studies [8].

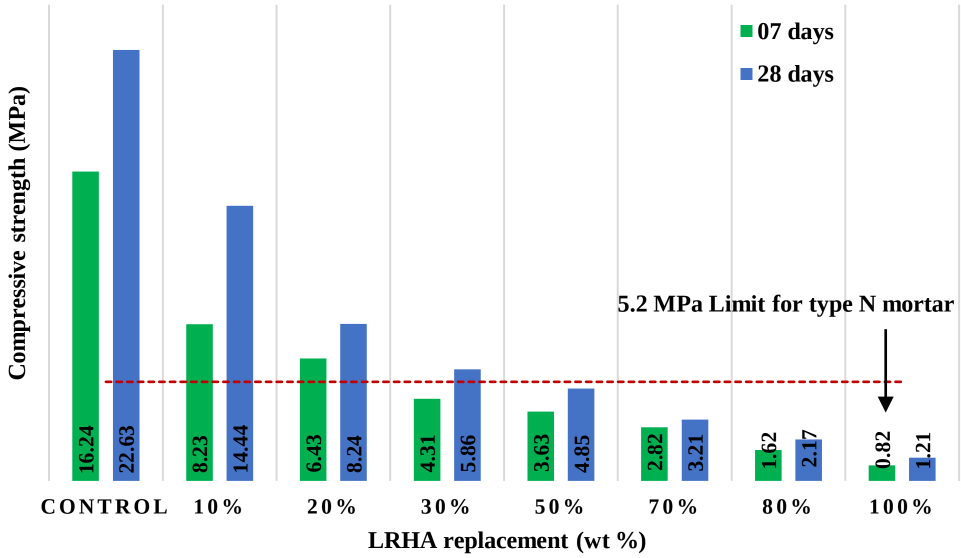

Figure 4.3: Compressive strength of samples with the different replacement of LRHA

4.3.3 Water absorption

Figure 4.4 shows the water absorption of developed mortar at different LRHA replacement. It is obvious that replacing natural sand with LRHA significantly increases the water absorption of mortar samples. The improvement in water absorption by 30% in the rice husk cement plaster, which is more than three times that of the control sample. It may be that there are more hygroscopic RHA particles. The decreased sand quantity would contribute to improved water absorption of LRHA cement, which is related to the rise of LRHA. Lower rates of LRHA substitution are directly related to the amount of porous LRHA particulate matter. The coarse particle nature of the LRHA cannot increase water resistance from either the pozzolanic effect or the effect of pore filling [54].

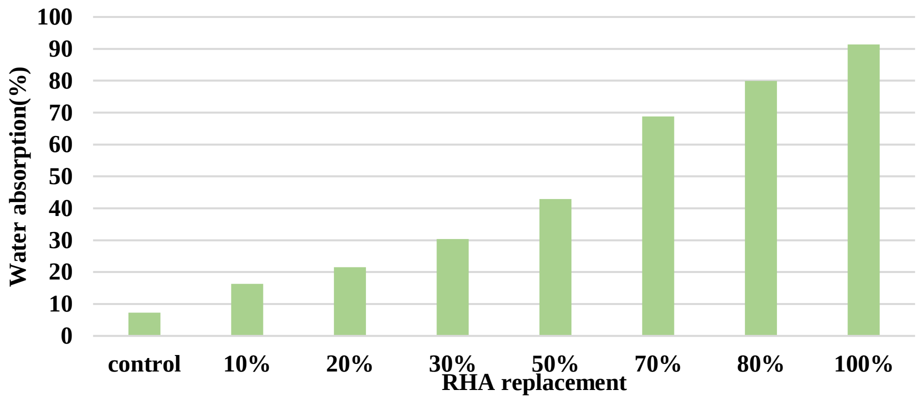

Figure 4.4: Water absorption of specimens with various amount of RHA replacement

4.3.4 Thermal conductivity

Figure 4.5 demonstrates the cooling curve and heating curve that is based on the heat flow theory from Lee's disc process.

$H = kA\ (T2 - T1\ )/x$ ....Eq 4.1

Where;

$$H\ =\ Steady\ state\ rate\ of\ heat\ transfer$$

$$k\ =\ Thermal\ conductivity\ of\ the\ sample$$

$$A\ =\ Cross\ sectional\ area\ of\ the\ sample$$

$$x\ =\ Sample\ thickness$$

$$(T2 - T1)\ =\ Temperature\ difference\ across\ sample\ thickness$$

$H = mc\ dT/dt$..Eq 4.2

Where;

$$m = Mass\ of\ the\ lower\ copper\ disc$$

$$c = Specific\ heat\ of\ copper$$

$$dT/dt = Heat\ radiated\ per\ second$$

By equating Eq (4.1) and Eq (4.2),

$mc\ dT/dt = kA\ ((T2 - T1))\ /x$..Eq 4.3

Sample calculation for MP-30-1,

Cooling curve gradient = Heat radiated per second = dT/dt = 0.01428 C/s

$$m = 880\ g$$

$$c = 0.385\ J/g\ ºC$$

$$mc\ dT/dt = 5.272$$

$$A = 0.002829\ m2$$

$$T2 - T1 = 40.4\ ºC$$

$$x = 0.005\ m$$

$$x/A\ (T\_2 - T\_1) = 0.0442$$

$$k = 0.210\ W/m$$

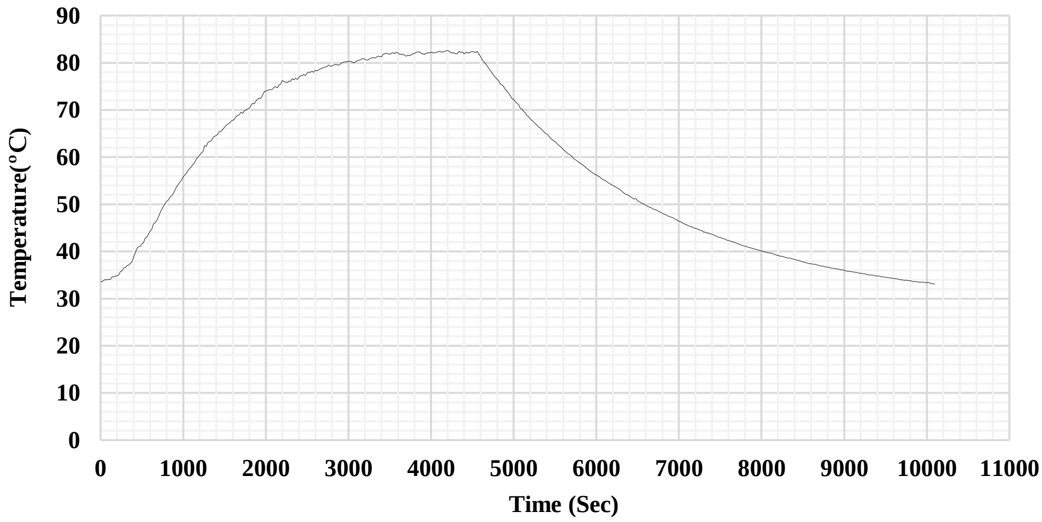

Figure 4.5: Data obtained from lee's disc method

Figure 4.6 and Table 4.3 shows the mortar's thermal conductivity with varying LRHA replacement rates. It is noteworthy that incorporating LRHA into the mortar matrix reduces the mortar's thermal conductivity which exhibited a property of good thermal insulator. Thermal conductivity values show a considerable decrease with increased LRHA content. The thermal conductivity of the 100% LRHA mortar was about 0.213 W /m K and it was about 0.824 W/m K for the control mix. This can be expressed as a reduction in thermal conductivity of 67.42% compared to the control mixt. The voids in the sample govern the thermal conductivity of porous materials [6].

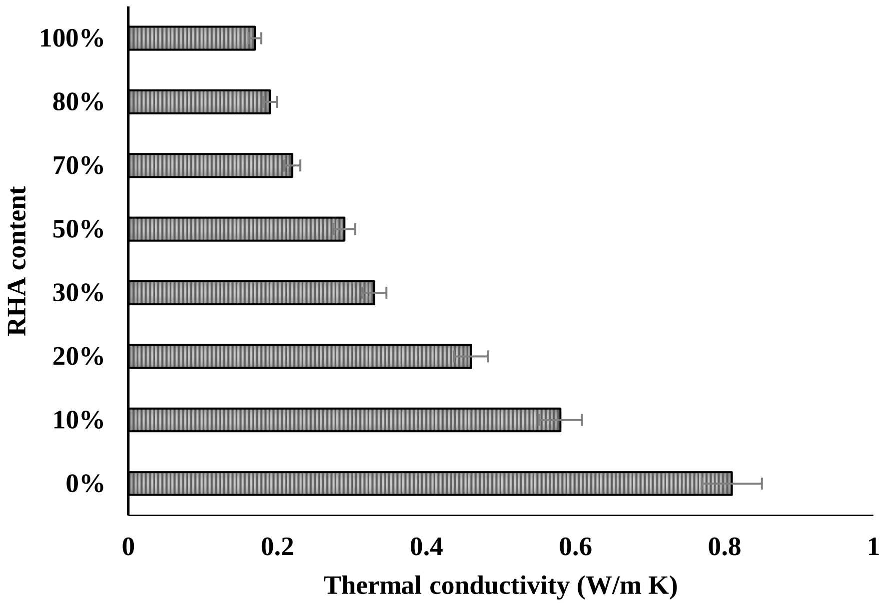

Figure 4.6: Relationship between the average thermal conductivity and amount of LRHA replacement

Table 4.3: Thermal conductivity values

Sample mix	**Thermal conductivity (W/m K)**
MX-0-1	0.824
MX-0-2	0.868
MX-10-1	0.384
MX-10-2	0.326

MX-20-1	0.302
MX-20-2	0.285
MX-30-1	0.210
MX-30-2	0.198
MX-50-1	0.182
MX-50-2	0.178
MX-70-1	0.174
MX-70-2	0.166
MX-80-1	0.146
MX-80-2	0.136
MX-100-1	0.132
MX-100-2	0.135

4.3.5 Density

The mortar density with RHA substitution variance at 28 days is shown in Figure 4.7. Weight and dimensions of cubes were measured. The result showed that the sample density with LRHA was lower than that of the samples under control. With the increase of LRHA replacement, both bulk density and dry density decreased. When the sand was completely replaced with RHA, the dry density of mortar was 0.6 g / cm^3 while the control sample was 2.2 g / cm^3 at 28 days of age. Low-density LRHA substituted with high-density sand and more water absorption are the two main reasons for the decrease of density by the creation of internal voids in mortars.

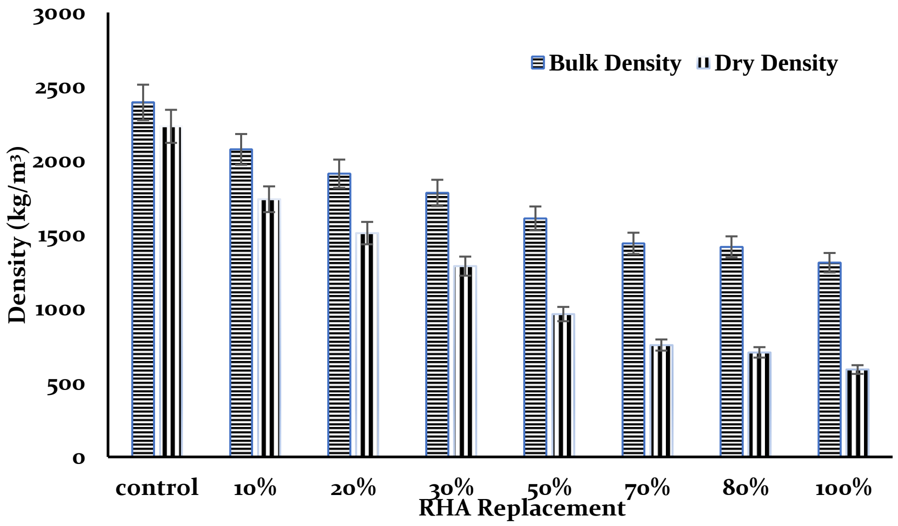

Figure 4.7: Bulk density and dry density variation of LRHA

4.3.6 Microstructure of RHA

SEM was used to analyze the microstructure of mortars comprising 10, 20, 30, 50, 70, and 100% LRHA and those are presented Figure 4.8. The SEM image of the control mortar without LRHA is shown in Figure 4.9. The control mortar was found to be denser than LRHA-containing mortar. With the rise in LRHA content, more pores were found. This can be explained by the excess water absorbed by the LRHA and this is the key explanation of why compressive strength is decreased.

It was observed that when the amount of LRHA increases, the amount of voids due to more water absorption by LRHA particles, also increases. As the water particles get evaporated more voids can be found, and the porosity also increases. When these voids are filled with air, it causes the reduction of thermal conductivity as the air has very low thermal conductivity.

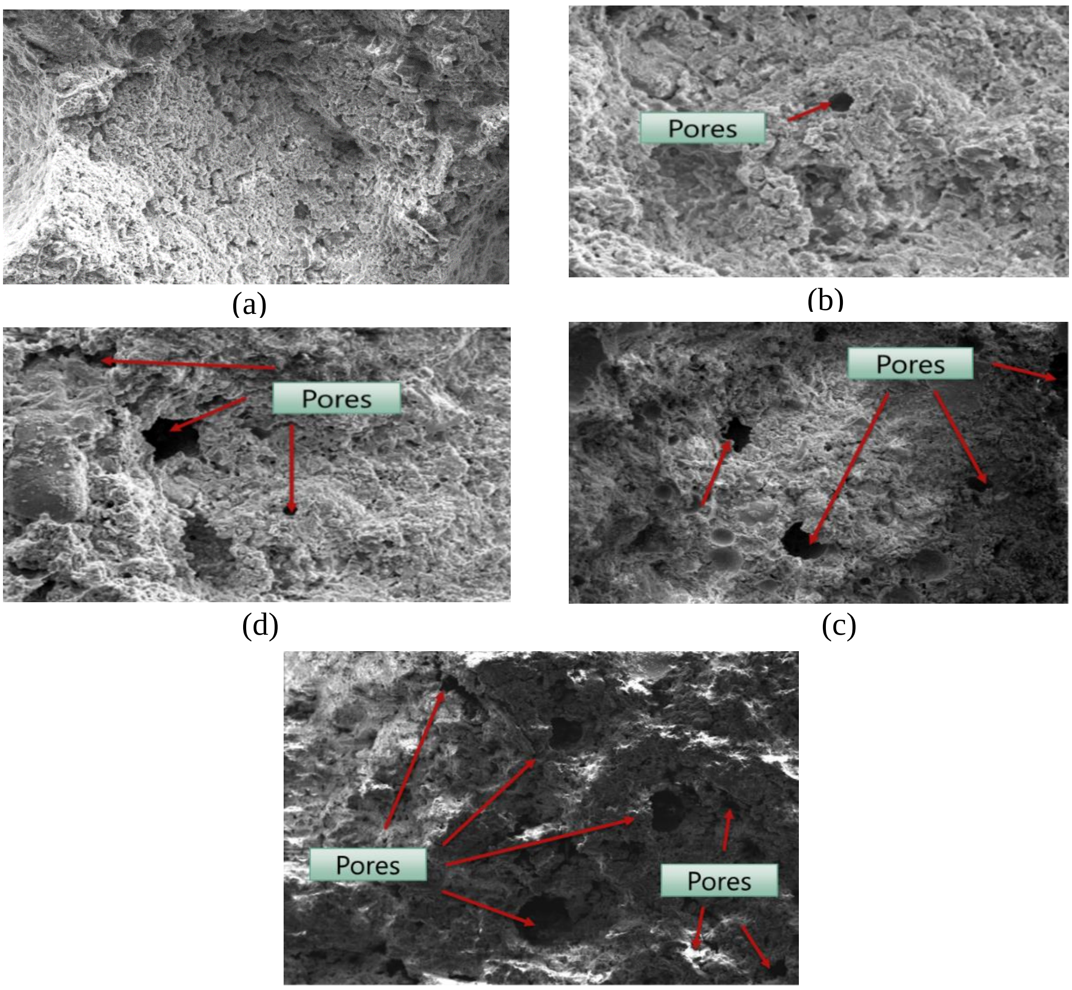

Figure 4.8: SEM image of mortar with Low-carbon RHA a) 20% b) 30% c) 50% d) 70% and e) 100%

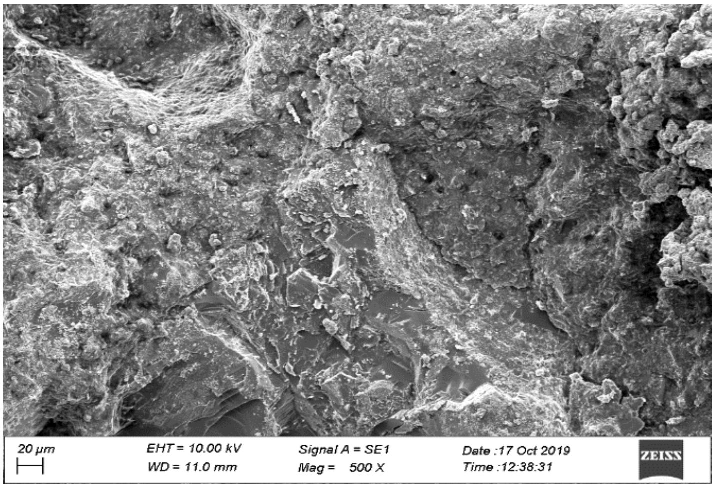

Figure 4.9: SEM image of mortar without RHA

4.3.7 Relationship between Thermal Conductivity and Density

Figure 4.10 shows the increment in dry density contributes to higher thermal conductivity. This is due to the reduction of the overall air-filled voids, whose thermal conductivity is lower than that of the matrix, thus accounting for the thermal conductivity effect of the dry mass. From these findings, it is clear that the less conductive composite was formed by the aggregates with less thermal conductivity. Earlier studies show that the composite form will have a major impact on the thermal conductivity of materials [35], [54], [55].

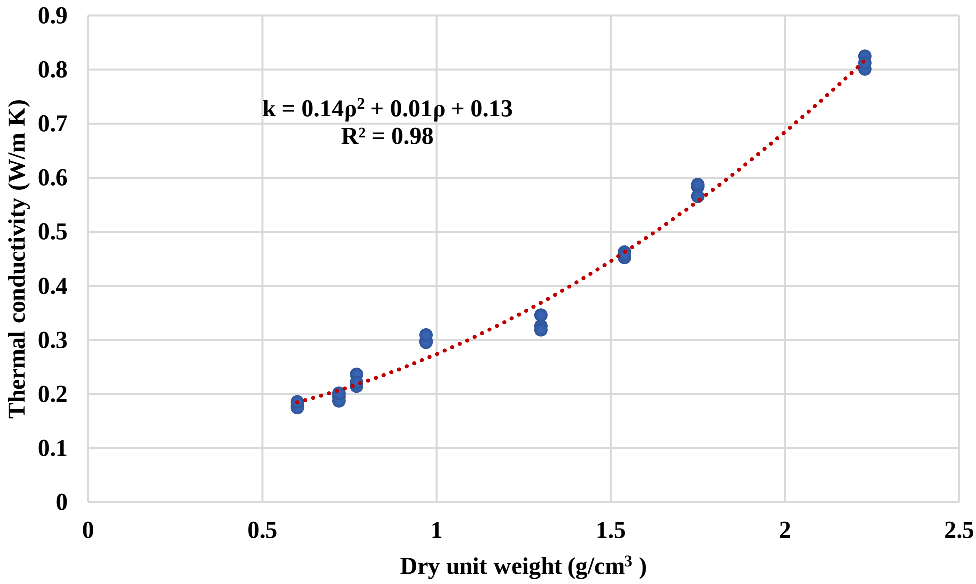

Figure 4.10: Thermal conductivity and density variation

Among all the specimens, the lowest thermal conductivity (0.178 W/m K) was obtained from the specimen with a dry density of 590 Kg/m^3.

The derived correlation was given in Eq 4.4:

$$k = 0.14\rho 2 + 0.01\rho + 0.13 \quad \text{...} \text{Eq 4.4}$$

The determination coefficient (0.9801) shows a relatively good thermal conductivity predictor. Meanwhile, it can also be inferred that density is a key thermal conductivity characteristic.

4.3.8 Relationship between Thermal Conductivity and Compressive strength

Figure 4.11 demonstrates the thermal conductivity and compressive strength of specimens of different densities. There is an increasing rise in thermal conductivity (k) with an improvement in compressive strength (f) resulting in a coefficient of correlation of $R^2 = 0.98$. The variance obtained is close to that recorded in preceding works [6], [13]. The relation of these two variables may be attributed indirectly to the density. The low-density specimen has lower porosity internally due to a higher pore volume, which decreases the heat transfer capacity across the specimen. Meanwhile, greater air-vacuums and a broader range of air-vacuum sizes in a low- density specimen result in reduced power. But the air-free distribution at high densities has little effect on the compressive strength, possibly due to higher density ranges having a more uniform distribution of voids (Figure 4.12(b)).

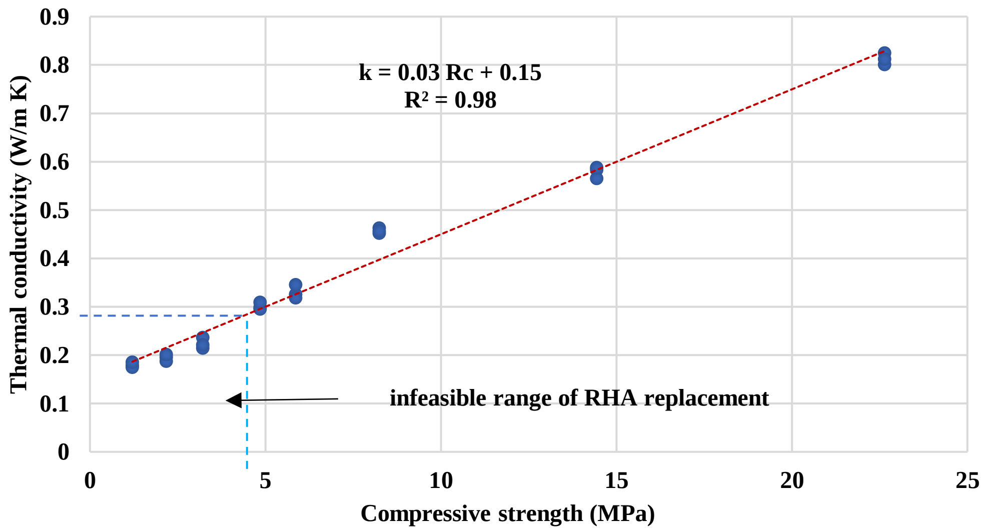

Figure 4.11: Variation of thermal conductivity with compressive strength

The relationship between thermal conductivity and dry density is confirmed to a polynomial pattern.

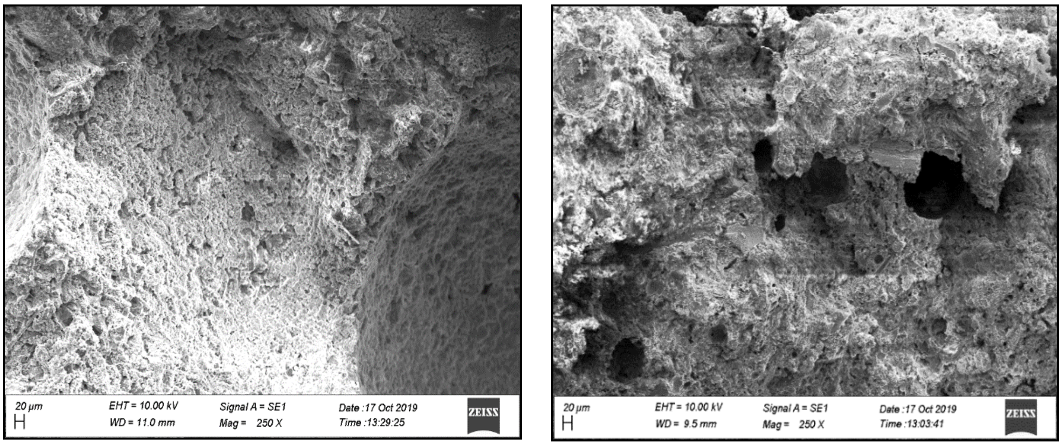

Figure 4.12: SEM image of mortar with (a) 10 % (b) 70 % RHA at ×250 magnification level

4.4 Conclusion

In this research, an experimental method was performed to test the thermal conductivity of mortar with LRHA. It has been found that this plaster will increase the buildings' thermal comfort and hence can be used as a good insulation plaster.

In addition, the influence of the compressive strength, density, water absorption, microstructure, and workability were tested, and the results suggested that it will be able to function as a proper insulation plaster.

4.5 High carbon RHA

HRHA was obtained by burning the rice husk in an open space for about 60 min [11] which is black in color (Figure 4.13). This chapter studies the mechanical and thermal properties of mortar incorporation with HRHA.

Figure 4.13: Raw rice husk before and after burning

4.6 Particle size distribution of LRHA

The particle size distribution of HRHA is presented in Figure 4.14. All the particles were passing through 500 µm. The particle size ranges from 0.15 µm to 500 µm.

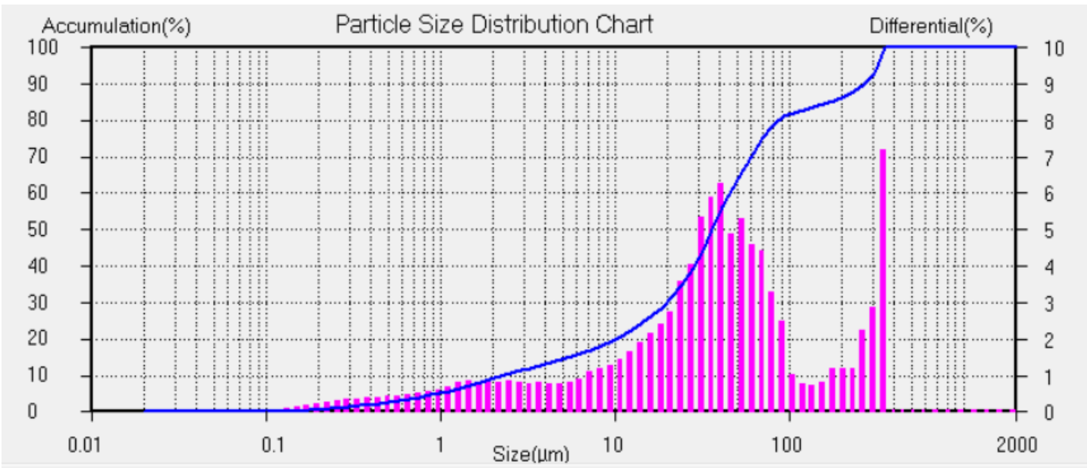

Figure 4.14: Particle size distribution of HRHA

The distribution curve of particle size for HRHA is given in Figure 4.14. The figure indicates that HRHA particles of large scale are approximately classified in contrast with cement particles. However, most of the particles are pairs of very small size with smaller particles than pairs of big scale, like normal sand.

Table 4.4 displays the particle properties of raw materials. Cement, RHA, and natural sand maximum particle sizes are 11.96 µm, 36.86 µm, and 0.86 mm, respectively. The findings were in line with finding of the previous research work.

Table 4.4: Raw material properties

Type of sample	Specific gravity	Average particle size d_{50}	Specific surface area (m^2/cm^3)
Cement	3.12	11.96 µm	0.725
HRHA	**2.18**	**36.86 µm**	**1.668**
Sand	2.62	0.86 mm	-

4.7 Chemical composition of HRHA

The chemical composition of the HRHA particles is listed in Table 4.5. This indicates that HRHA contains 51.2 % of SiO_2 which does not satisfy the limit for the F type pozzolans with ASTM C618 [11].

Table 4.5: Raw materials chemical composition

Materials	Chemical properties, Oxide compositions (wt%)								
	SiO_2	Al_2O_3	Fe_2O_3	CaO	MgO	Na_2O	K_2O	SO_3	LOI
OPC	19.03	4.21	3.16	66.06	2.54	-	0.34	2.74	2.11
HRHA	**51.2**	**0.3**	**0.3**	**2.8**	**1.4**	**0.8**	**3.4**	**0.68**	**39.12**
Sand	93.42	2.41	1.51	0.41	0.10	0.10	0.90	-	0.68

4.8 Microstructure and morphology of materials

Figure 4.15 displays an overview of HRHA nature, as observed by scanning electron microscope (SEM). The HRHA is slightly angular as seen from the SEM images, with a finer texture on the top.

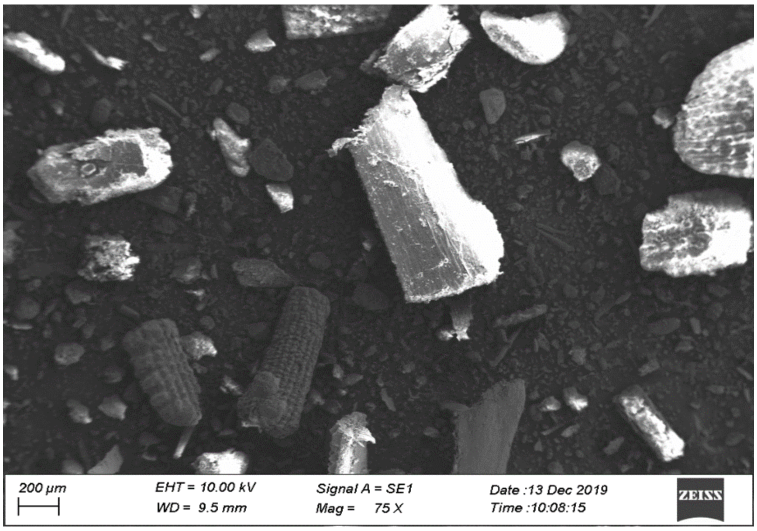

Figure 4.15: SEM observation of HRHA at × 75 magnification level

Despite of the higher basic surface area, the HRHA microstructure is very porous and spongy. The HRHA particles are distributed with different particle sizes over a wide size spectrum. Additionally, the HRHA particles tend to be circular, vesicular, and coated with a porous microstructure. HRHA's SEM findings clearly contradicts previous studies [56].

4.9 Properties of HRHA incorporated Mortar cubes (Preliminary study)

4.9.1 Workability

Results show that a reduction in flow when compared to the control sample as the RHA percentage increases, due to its high surface area which needs greater water requirement. The mixture flow without HRHA was 140 mm, while mixture flow was 100 mm with 20% of HRHA being replaced with sand. If it goes above 30% there is no flow which means the needed water is not enough to get the same flow with the same 0.5 w/c ratio. This study specifically shows a decrease in flowability with the increase of the HRHA. In previous research, related trends have been identified. Therefore, it can be inferred that more water is required to ensure the proper flowability of the mixture with the HRHA. The increased demand for water can be due to the tiny porous and spongy nature of HRHA which may contribute to a rise in the HRHA surface area.

The water demand for mortars containing HRHA grow with the increase in the HRHA %. The additional need for water is because of the extremely wide surface area of the HRHA particles, which must be wetted.

4.9.2 Compressive Strength

The compressive strength of HRHA-containing mortar is shown in Figure 4.16. From the figure, it can be concluded that the increase of HRHA percentage results in the reduction of both 7 days and 28 days strength.

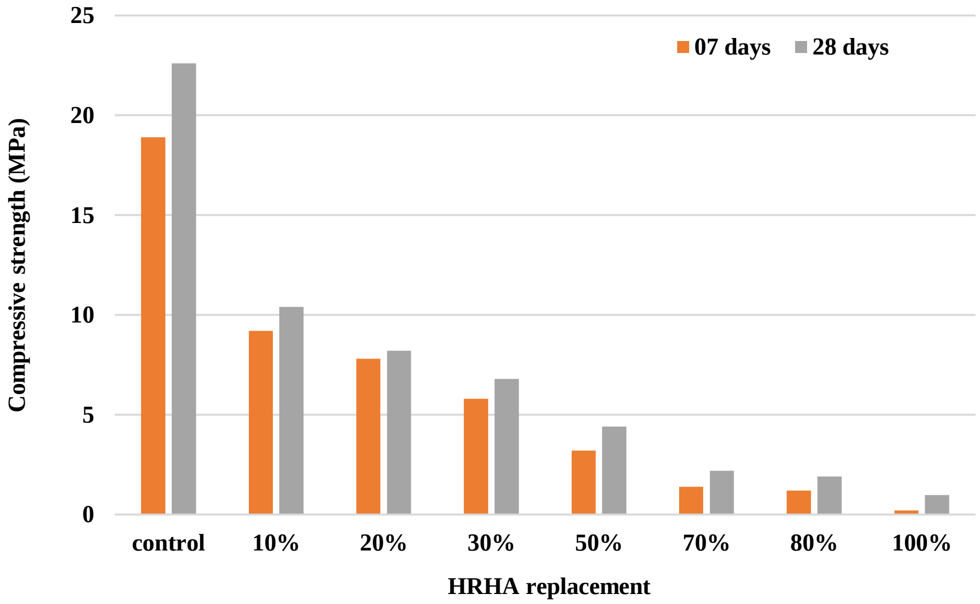

Figure 4.16: Compressive Strength with various RHA

The reason for the reduction in the compressive strength is the insufficient bonding of HRHA within the mixture which is due to its coarse nature which ends up in creating more porosity. The main reason for the strength is the presence of SiO_2 in the form of amorphous. When cement is reacted with water, the produced calcium hydroxide reacts with amorphous silica resulting in CSH hydrates being produced. The main reason for compressive strength is in CSH hydrates. However, if the amount of cement remains the same, the explanation for the drop in strength is the reduction in the sand and the increase in pores.

The compressive strength of mortar is found to significantly decrease with the rise of HRHA. Mortar containing 10, 20, 30 and, 50% HRHA shows significant compressive strength while sand replacement with HRHA above 50% shows a huge reduction of compressive strength which does not satisfy the limit of ASTM C270 which is 5.2 MPa [57]. The specimen's maximum compressive strength with 50 % HRHA substitution is 4.8 MPa, less than the required standard. Hence, this activity is attributed to the introduction of low-density RHA that results in increased mortar porosity.

4.9.3 Water absorption

As predicted, the mortar containing HRHA was higher in water absorption than the mortar blocks. Like control cubes, this can be due to the extremely porous nature of mortar containers with RHA. Figure 4.17 indicates the water absorption levels at the various replacement of RHA for the mortar blocks.

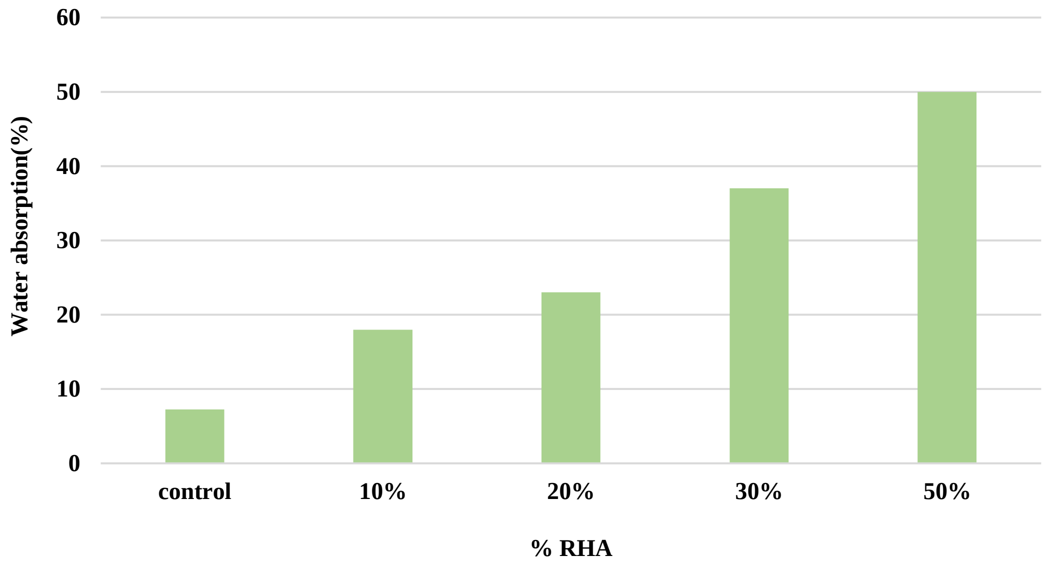

Figure 4.17: Relationship between water absorption and amount of RHA

4.9.4 Thermal conductivity

Figure 4.18 shows the cooling curve and heating curve from Lee's Disc method which is based on the principle of heat flow.

$H = kA\ (T2 - T1\ )/$...Eq 5.1

Where;

$$H\ =\ Steady\ state\ rate\ of\ heat\ transfer$$

$$k\ =\ thermal\ conductivity\ of\ the\ sample$$

$$A\ =\ Cross\ sectional\ area\ of\ the\ sample$$

$$x\ =\ Sample\ thickness$$

$$(T2 - T1) =\ Temperature\ difference\ across\ sample\ thickness$$

Here

Figure 5.1: Data obtained from lee's disc method

$H = mcdT/$
dt...Eq 5.2

Where;

$$m\ =\ Mass\ of\ the\ lower\ copper\ disc$$

$$c\ =\ Specific\ heat\ of\ copper$$

$$\frac{dT}{dt} =\ Heat\ radiated\ per\ second$$

By equating Equation (5.4) and Equation (5.5),

$mc\ dT/dt =\ kA\ (T2 - T1)\ /x$..Eq 5.3

Sample calculation for MP-30-2,

Cooling curve gradient = Heat radiated per second = dT/dt = 0.01428 C/s

$$m\ =\ 880\ g$$

$$c\ =\ 0.385\ J/g\ ºC$$

$$mc\ dT/dt = 4.541$$

$$A = 0.002829\ m2$$

$$T2 - T1 = 72.2\ ºC$$

$$x = 0.005\ m$$

$$x/A\ (T\_2 - T\_1) = 0.0524$$

$$k = 0.246\ W/m\ K$$

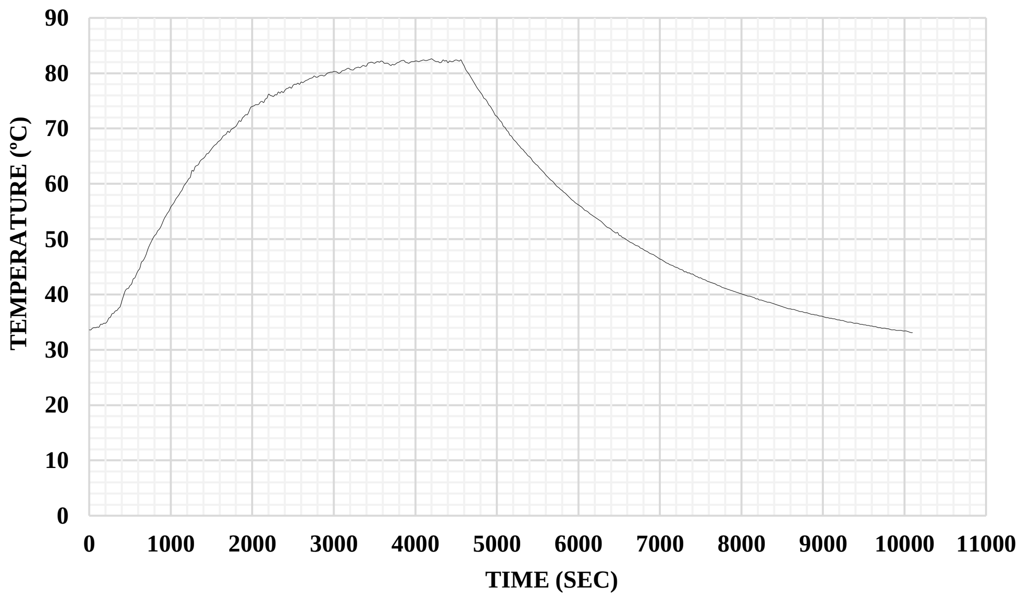

Figure 4.18: The cooling curve and heating curve from Lee's Disc method

Figure 4.19 and Table 4.6 shows the mortar's thermal conductivity with differing HRHA replacement rates. It is noteworthy that incorporating HRHA into the mortar matrix decreases the mortar's thermal conductivity which exhibited a strong property of thermal insulation. Thermal conductivity values display a significant decrease with increased HRHA content. The thermal conductivity of the 100% HRHA mortar was around 0.201 W/m K. It can be expressed as a decrease in thermal conductivity of 75.60 % relative to the control mixture. When the sand was completely replaced with RHA, the dry mortar density was 0.55 g/cm^3 while that of the control sample was 2.2 g/cm^3 at 28 days of age.

Table 4.6: Thermal conductivity values of samples

Sample mix	Thermal conductivity (W/m K)
MX-0-1	0.824
MX-0-2	0.868
MX-10-1	0.396
MX-10-2	0.365
MX-20-1	0.312
MX-20-2	0.308
MX-30-1	0.235
MX-30-2	0.246
MX-50-1	0.226
MX-50-2	0.218
MX-70-1	0.229
MX-70-2	0.226
MX-80-1	0.214
MX-80-2	0.208
MX-100-1	0.205
MX-100-2	0.198

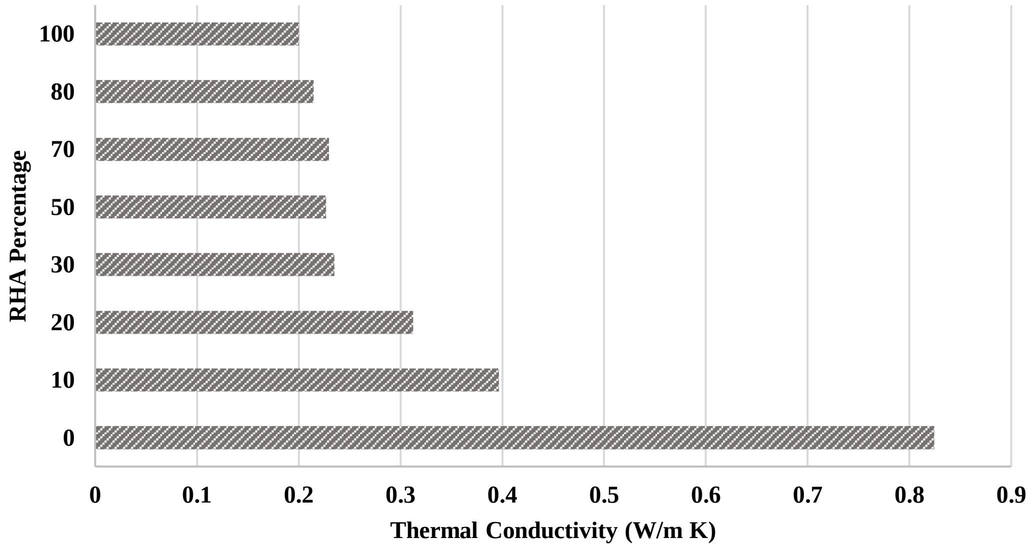

Figure 4.19: Relationship between the average thermal conductivity and amount of HRHA replacement

4.9.5 Density

The mortar density variation after 28-days with the HRHA replacement is shown in Figure 4.20. The result revealed that the sample density with RHA was lower than that of the samples under observation. With the rise in RHA substitution, both bulk density and dry density decreased.

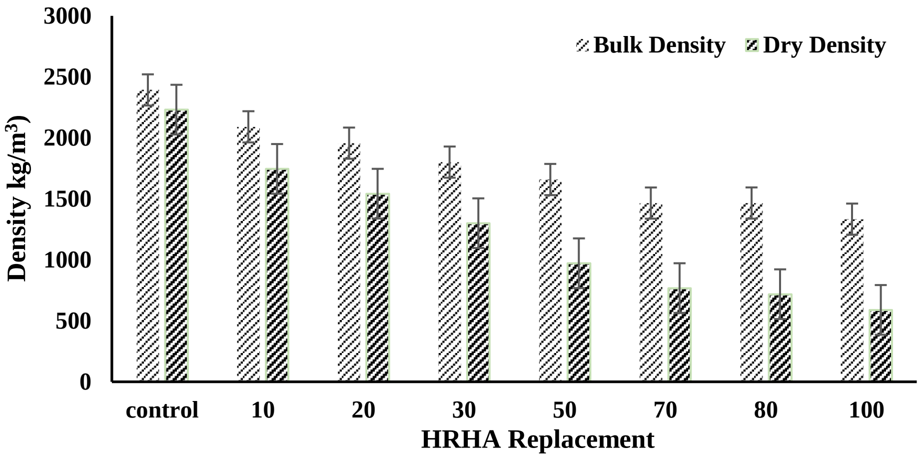

Figure 4.20: Bulk density and dry density variation of HRHA

4.10 Microstructure of HRHA

The microstructure of mortars containing 20, 30, 50, and 100% of HRHA are shown in Figure 4.21. When comparing with mortar without HRHA, it can be concluded that more pores are revealed. More pores were observed with the increase of HRHA content.

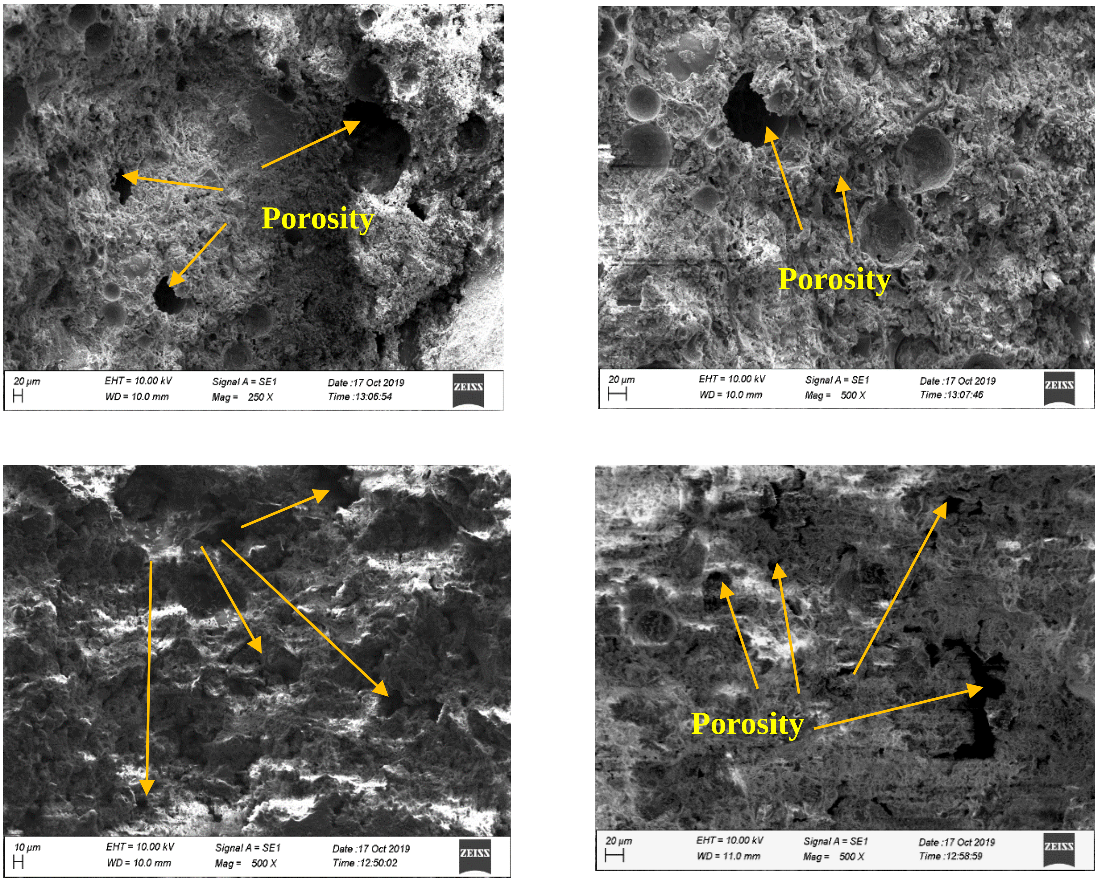

Figure 4.21: SEM images of mortars containing (a) 20 %, (b) 30 %, (c) 50 % and (d) 100 % of HRHA

This can be explained that the water absorption rate of HRHA is more than the control one. When the water gets evaporated, this leads to more voids, which is the main reason for the reduction of compressive strength and an increase in thermal conductivity.

4.11 Conclusion

An experimental system program to investigate the thermal behaviour of HRHA mortar has been performed. Cement-based plaster, which is made of rice husk ash as the base materials, was developed at University of Moratuwa. The thermal comfort of the buildings may be enhanced by this plaster. The effect of compressive strength, density, absorption of water, microstructure, and plaster flowability were examined, and the results proved that it will be able to function as a strong insulation plaster characteristic.

4.12 Comparative study on LRHA and HRHA mortar

Table 4.7 indicates that LRHA has a smaller average particle size than the HRHA, as also seen from the of particle size distribution. Since these samples were generated in a controlled environment, this result was predicted. With the increase of the grinding time, the average RHA particle size decreases significantly. Average RHA particle size is larger than OPC is unable to participate effectively in a pozzolanic reaction as in the previous studies due to inadequate grinding, which is one explanation for the compression strength reduction when substituted by fine aggregates.

Table 4.7: Comparison of average particle size

Type of sample	Average particle size d_{50} (μm)
LRHA	21.37
HRHA	36.86

4.13 Chemical analysis

Table 4.8 indicates the relation between LRHA and HRHA chemical composition. The LRHA contains more silica than HRHA due to improper HRHA burning conditions as seen in Table 4.8. It is confirmed that the greater loss of ignition for HRHA produces more unburned carbon particles. The quantity of SiO_2 in RHA is the key factor in the effectiveness of the pozzolan substance. By comparing both samples LRHA can be concluded to be more efficient than HRHA pozzolan content.

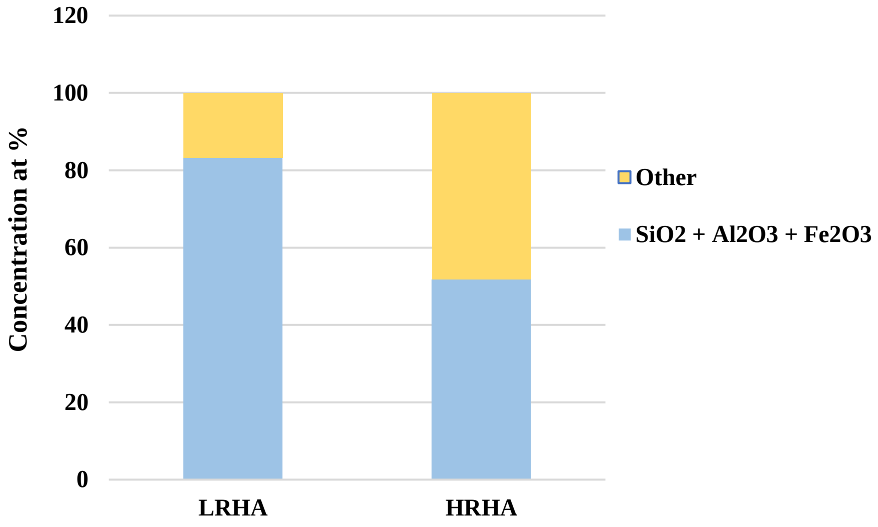

Figure 4.22: Chemical composition of rice husk ash samples

A pozzolan is graded as F pozzolans, as per the ASTM C618 [51], if the total number of SiO_2, Al_2O_3, and Fe_2O_3 exceeds 70%. In this study, as shown in Figure 4.22, the LRHA (SiO_2 + Al_2O_3 + Fe_2O_3) oxide concentration averages over 70%. And the amount of oxides in HRHA is less than 70% but greater than the minimum level (50 %) defined as class C pozzolana in ASTM C618 [51], but in this case, it may be considered as F pozzolans.

Table 4.8: Chemical composition of materials

Chemical composition (%)	LRHA	HRHA
SiO_2	81.4	51.2
Al_2O_3	1.10	0.3
Fe_2O_3	0.70	0.3
CaO	2.60	2.8
MgO	1.10	1.4
Na_2O	0.30	0.8
K_2O	0.60	3.4
SO_3	0.96	0.68

LOI	5.80	39.12

Further, both LRHA and HRHA contain less than 4% of sulfur trioxide (SO_3) which corresponds to the maximum permissible ASTM C618 limit [24]. The use of fertilizers is primarily attributed to the use of LRHA in the presence of K_2O in rice crops (not more than 3%). LRHA can, therefore, be graded as pozzolan Category F. Nonetheless, for HRHA, the K_2O rate is more than 3%. The claims concerning the chemical characteristics of RHA are consistent with the findings already published [21], [48], [58].

4.14 Microstructure and morphology of materials

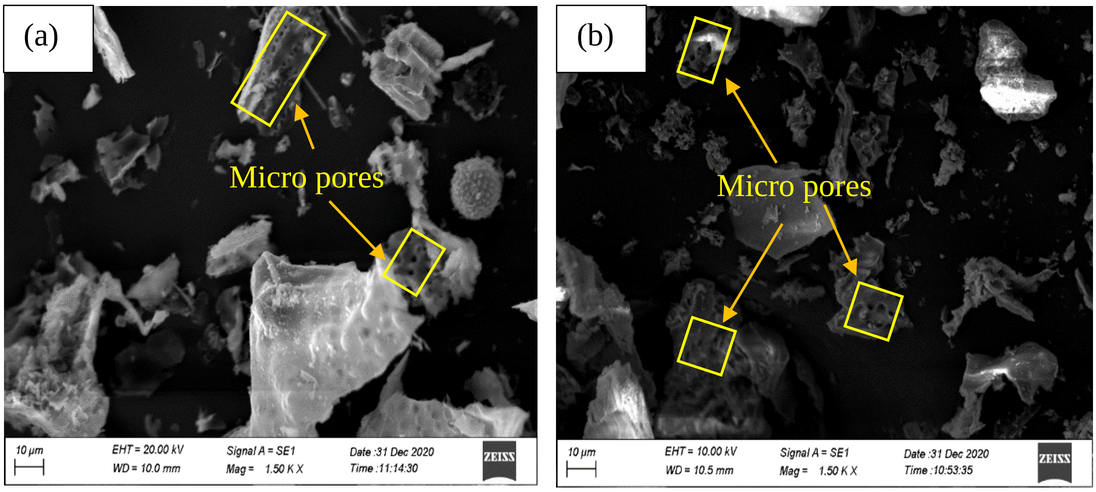

Figure 4.23: SEM observation of (a) LRHA (b) HRHA at × 75 magnification level

Figure 4.23 (a) and (b) show SEM images of both LRHA and HRHA. As these figures demonstrate, due to the highly variable surface area, the microstructure of LRHA and HRHA is very porous and spongy. The HRHA particles are scattered across a wide range of dimensions, while the LRHA component size range distributed broadly with cell, angular, and sponge particles. In addition, irregular, vesicular, and the porous microstructure is typically found on HRHA particles. The LRHA particles cluster many smaller particles comparatively better. Higher rates of small RHA particles are required to ensure that the pozzolan reaction is successfully involved.

4.15 Conclusion

The comparative analysis between LRHA and HRHA was discussed in this chapter. Studies indicate that LRHA is more pozzolanic than HRHA as it is known as F pozzolan containing more silica. LRHA mortar has stronger mechanical and thermal properties than HRHA mortar. Therefore, the incorporation of low carbon RHA into mortar proved to be feasible for thermal insulation plaster development, mainly because the properties investigated have fair efficiency. But in case of thermal conductivity, if the compressive strength is not important, HRHA can be used as good insulation material.

CHAPTER 5: IMPROVEMENT OF MECHANICAL PROPERTIES AND ECONOMIC ANALYSIS

5.1 Overview

From Chapter 5, it was evident that LRHA particles show good mechanical properties than HRHA particles. The flow and compressive strength of the mortar with RHA particles above 30 % replacement shows a drastic reduction. Therefore, compressive strength testing was repeated by adding superplasticizers for the 30 % and 40 % replacement of RHA in the mixture.

5.2 Results and discussion

One of the objectives of this experiment was to decrease the water-cement ratio by using chemical admixtures. The mix proportions details are given in Table 5.1.

Table 5.1: Mix proportion of mortars containing different RHA replacement.

Sand replacement	**Low-carbon RHA**				
	Cement (kg)	Sand (kg)	RHA (kg)	Superplasticizer (ml/kg of cement)	Water(kg)
30%	1.0	1.2	1.8	10	0.86
40%	1.0	1.5	1.5	10	1.24

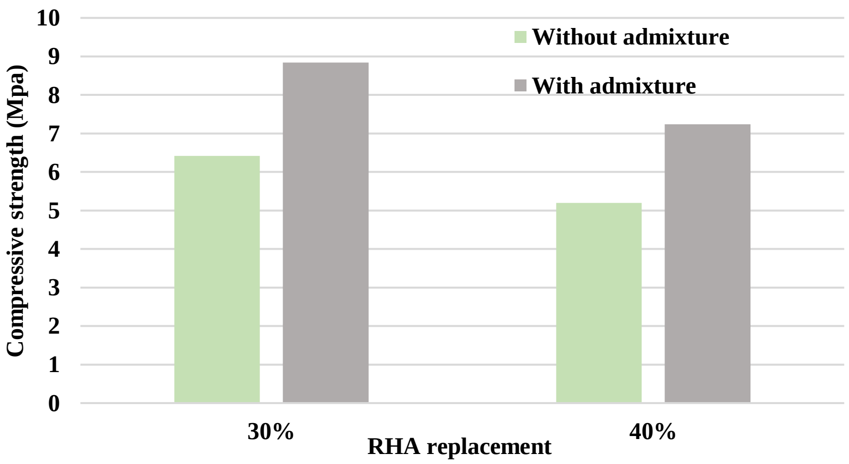

Figure 5.1: Comparison of compressive strength with super plasticizer in Low-carbon RHA mortar

Table 5.2: Properties of the sample with super plasticizer

Sample	w/c ratio	Superplasticizer (ml/kg of cement)	Average compressive strength (MPa)	Average density (kg/m^3)	Average Flow (mm)	Average thermal conductivity (W/m K)
RHA30	0.96	10	8.84	1705	135	0.212
RHA40	1.12	10	7.23	1580	125	0.197

The workability of the mortar prepared with plasticizer is decreased when compared to previous studies without plasticizer as shown in Table 5.2. Figure 5.1 shows the variation of 28 days compressive strength.

5.3 Economic analysis

In Sri Lanka, annual paddy production is 3.65 million metric tons. Annual rice husk production is 3.65*0.20 million metric tons which means 0.73 million metric tons: assuming husk from 20% of paddy grain in weight. Annual RHA production in Sri Lanka is 0.73*0.20 which means 0.146 million metric tons, assuming husks when burnt reduces in weight to 20% of husk weight. This estimate considered the transportation cost to University of Moratuwa. Transport expenses for cement and sand from plants in Ratmalana and Mount Lavinia were also estimated. Because transport costs may vary with time and means of transport and the cost for rice husk ash be considered as zero which is freely available, and it is collected from Panadura. Direct cost is the inclusion of transport costs and material costs given in Table 5.3.

Table 5.3:Market prices of materials

Material	Quantity	Direct cost (LKR)
Cement	1 Bag	960
Sand	12 m^3	35000
Rice Husk Ash	10 m^3	3000

The bill of quantities details was given in Table 5.4. The cost of the Vermitex ® TH for 50 liters is 1,020,000 LKR according to the year 2019.

Table 5.4: Bill of Quantities

Material	Unit	Unit price (LKR)	Conventional plaster		RHA plaster	
			Quantity	Cost (LKR)	Quantity	Cost (LKR)
Cement	1 m^3	59850.00	1 m^3	59850.00	1 m^3	59850.00
Sand	1 m^3	2915.00	3 m^3	8475.00	2.5 m^3	7287.50
RHA	1 m^3	300.00	-	-	0.5 m^3	150.00
Total cost for 1 m^3 plaster				17081.25		16821.87

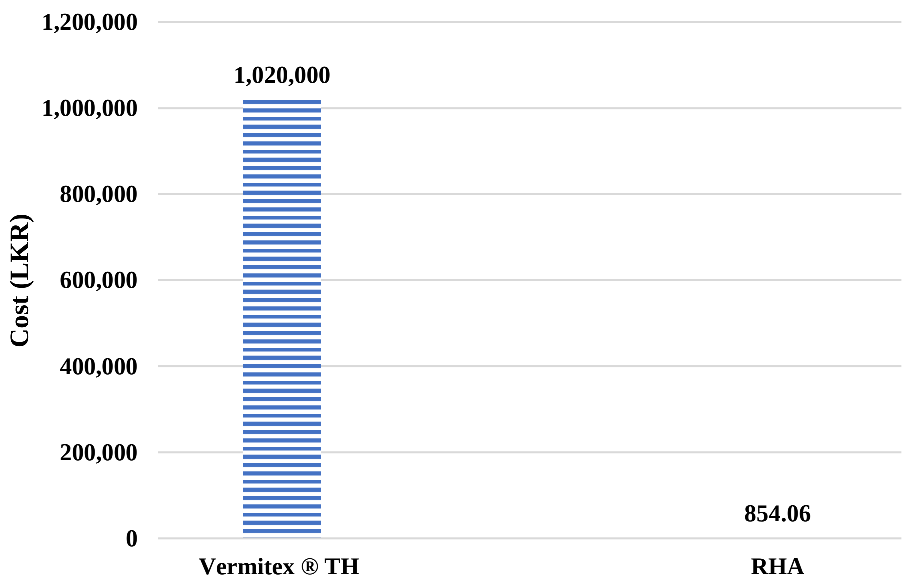

Figure 5.2: Cost comparison of Vermitex and RHA plaster

Figure 5.2 shows the comparison of the product available in the market (Vermitex ® TH) and the invented product. RHA plaster is recommended as a very cheap product that nearly has the same mechanical properties. If this product can be introduced to the industry, we can save a lot of money.

5.4 Comparison of developed mortar with commercially available product

The main objective of this project is the production of low-cost CFRP isolation mortar from waste material. Vermitex ® TH is a commonly used commodity on the market as a CFRP EPOXY fire safety plaster. Vermitex ® TH is a cement-vermiculite coating specifically formulated for hydro-carbon fires for structural steel, concrete, and other substrates. Vermitex TH is easy to use and asbestos-free. It is manufactured to ensure consistency and cost-efficient lacquers, typically without mechanical reinforcement of concrete substrates, that can be applied with a spray gun in normal circumstances [35].

Vermitex ® TH is a lightweight coating made from extended vermiculite and inorganic binders of acceptable thickness. The air-training system creates huge quantities of micro-dispersed air bubbles during the mixing process. It ensures high fire resistance and decreases thermal conductivity.

Vermitex ® TH combines excellent properties of fire and thermal insulation with noise reduction and anti-condensation. Vermitex ® TH is particularly designed for hydrocarbon fire safety and extensively tested to meet the UK and Australian standards. Thermal conductivity of 0.114 W / m K can be applied to the thicknesses between 15 and 20 mm in one test, and the fire resistance levels are from 30 (30) to 4 (4) hours.

The invented product which is known as "**AGRO Mortar**" using RHA seems to have better thermal insulation property as shown in Figure 5.3. Vermitex is a trending product in the market, which is very costly, so introducing Agro mortar to the industry will help to reduce the cost and helps to reduce the environmental effect of sending RHA waste to the landfills.

Table 5.5: Comparison between Vermitex and Agro mortar at 25 °C

	Vermitex ® TH	**Agro Mortar**
Appearance	Gray nominal	Gray colour Powder
Max aggregate size	-	2 mm
Application thickness	10-50 mm	10- 30 mm
Dry hardened density	400 kg/m^3	850 kg/m^3
Wet density	590 kg/m^3	1600 kg/m^3
Pot life @ 25 °C	4 Hours	2.5 Hours Approx.
Compressive strength @ 28 day	48 kPa	5-10 MPa
Thermal conductivity	0.114 W/m K	0.2-0.3 W/m K
Flow	-	140 mm
Water Absorption	-	$\leq$ 0.85 kg/m^2

5.5 Chapter summary

This chapter addressed the experiments with plasticizers for selected LRHA mortar samples. The studies suggest that 40% of LRHA mortar samples are a revolutionary mixing method with good mechanical and thermal properties. Finally, LRHA is successfully manufactured with lightweight insulating material with excellent results. From the preliminary cost analysis performed in this chapter, it is clear that using the RHA plaster developed in this study would be cost-effective while providing additional thermal comfort to the buildings.

CHAPTER 6: LIFE CYCLE ASSESSMENT (LCA) OF RHA-ASED MORTAR

6.1 Overview

The environmental sustainability of RHA-based mortars that to be used in the building profile as plastering material, life cycle assessment (LCA) was carried for the trialled mortar mixes in this research. The LCA study was conducted to compare the environmental impact of producing 1 kg of mortar as a functional unit with 8 different mix-design using RHA (Table 6.1). The process started with raw material processing and ended with the transportation of the final products. A "cradle to gate" boundary was considered in this research that comprises of various stages such as extraction of material (i.e., each extraction of raw material, transport), manufacturing stage that involves processing and testing, and supply stage of the product excluding treatment and disposal phases.

The inventory of the LCA was developed to produce a plastering mortar with low thermal conductivity and a minimum compressive strength of 5.2 N/mm^2 accordance with ASTMC270 [59]. The impact assessment is generated with the LCA software SimaPro 8.2.0.0 [60] using Recipe Midpoint (H)/ World Recipe H method [61]–[63]. This tool was used to collect, model, and translate the life-cycle inventory data into environmental impacts. This method has the broadest sent of midpoint categories and generates 18 midpoint impact categories (i.e. climate change, ozone depletion, terrestrial acidification, freshwater eutrophication, marine eutrophication, human toxicity, photochemical oxidant formation potential, particulate matter, terrestrial ecotoxicity, marine ecotoxicity, Ionising radiation, agricultural land occupation, urban land occupation, nature land transformation, water depletion, metal depletion, and fossil depletion).

The system boundary of this LCA follows the AS ISO 14040:2019 [64] and EN 15978 [65] (Figure 6.1). Figure 10 shows that this LCA included cement production, aggregates excavation, water supply, and source material into consideration during the material extraction stage. The transportation of materials is also included in this LCA.

The distance between the various locations was calculated by the road mapping software based on real life data. The travel distance of transport product to clients was assumed to be 50 km. All the location distances are measured from University of Moratuwa, Sri Lanka. In the production stage, the energy consumption of the mortar production is consisting of two parts, mixing, and testing. The energy consumption of mixing (i.e. 2.2 kWh/kg) and testing (1.35 kWh/kg) was calculated from the lab experiments. The transportation of the final product to the client is considered as final stage of this LCA analysis.

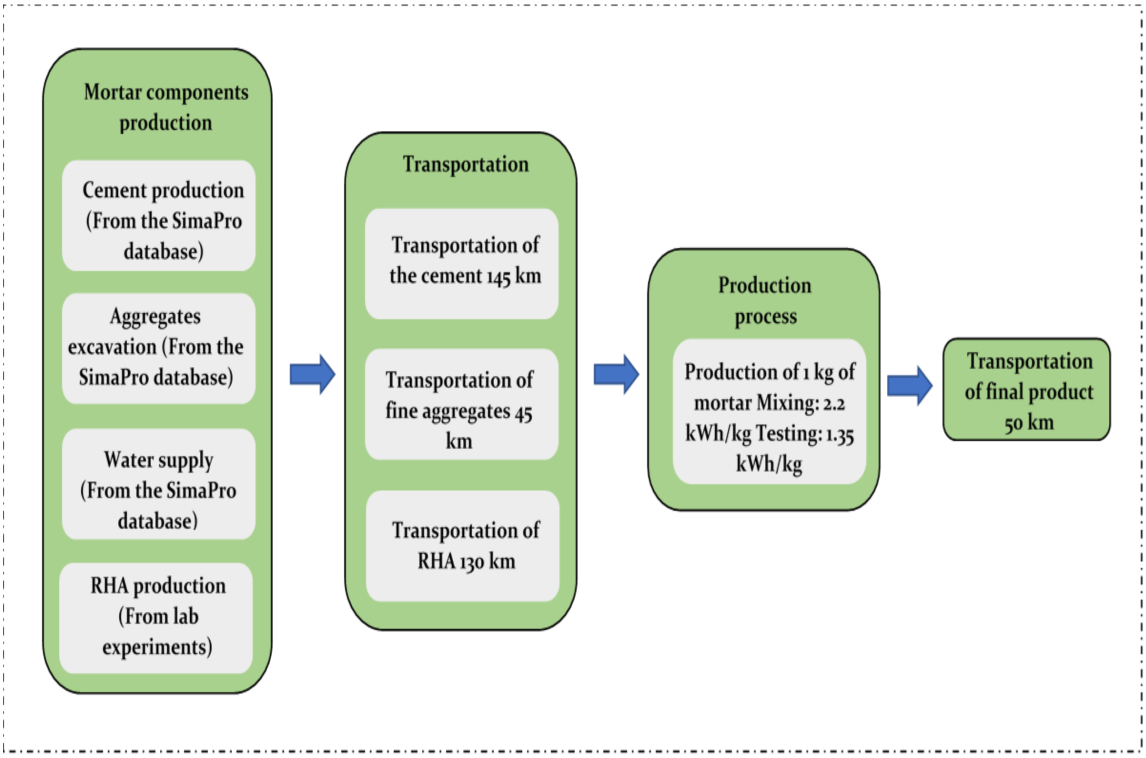

Figure 6.1: The system boundary of the LCA study of eight mortar mix design

Table 6.1: Mix design of the mortars replaced with various amount of RHA

	Mixtures (g)							
Materials	**M0**	**M1**	**M2**	**M3**	**M4**	**M5**	**M6**	**M7**
Cement	222.3	213.6	207.5	191	167.8	160.4	149.7	141.6
Sand	666.3	576.8	498	401	251.7	144.3	90	-
Water	111.1	145.4	170	236.1	328.7	358.6	400.9	433.5
RHA	-	64.1	124.5	171.8	251.7	336.7	359.3	424.8

6.2 Environmental impact on the production of RHA-based mortar

Results of impact categories climate change, ozone depletion, human toxicity, terrestrial acidification, freshwater ecotoxicity, fossil depletion are presented in this section. These impact categories relate to the impact of human health (climate change, ozone depletion, and human toxicity), damage to ecosystems (terrestrial acidification, and freshwater ecotoxicity) and damage to resource availability (fossil depletion). Figure 8.2 shows the mortar production impact on climate change, which is CO_2 equivalent. This figure shows that the mix design M0, where there is no substitution of waste material has the highest impact in climate change (i.e. 1.34 kg of CO_2 gas emission). The increase in the RHA amount significantly reduces the climate change impact as the CO_2 emission is reducing when the mortar mix replaced by RHA of 10% (i.e. M1) shows a 9% reduction in CO_2 emission. This reduction was further reduced by 5%, 8%, 12% and 15% when increasing the RHA contents to 30%, 50%, 70% and 80%. A 100 % sand replaced by RHA in the mortar reduce the CO_2 by 26% in comparison with reference (i.e. M0). The decrease due to the use of less quantity high carbon intensive cement in RHA-based mortar, when compared to the M0.

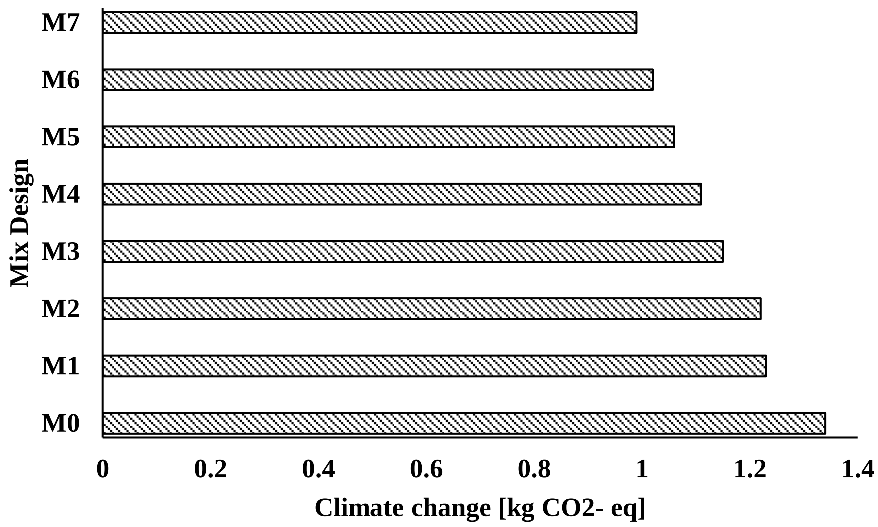

Figure 6.2: Impact of climate change

The ozone depletion from the production of RHA-based mortar is presented in Figure 6.3 and the indicator of these impact categories was presented by trichlorofluoromethane (CFC-11) equivalent. This figure shows that the mix design M0 has the highest impact in ozone depletion with 7.81E-09 kg of CFC-11. The impact of ozone depletion was reduced by 6% when the RHA contents increased from 0% (i.e. M0) to 30% (i.e. M3) in the mortar. Further, the mix proportions with more than 50% of substitution of RHA could be highly recommended as it gives a significant reduction of ozone depletion, in the range of 10.62%-14.85%.

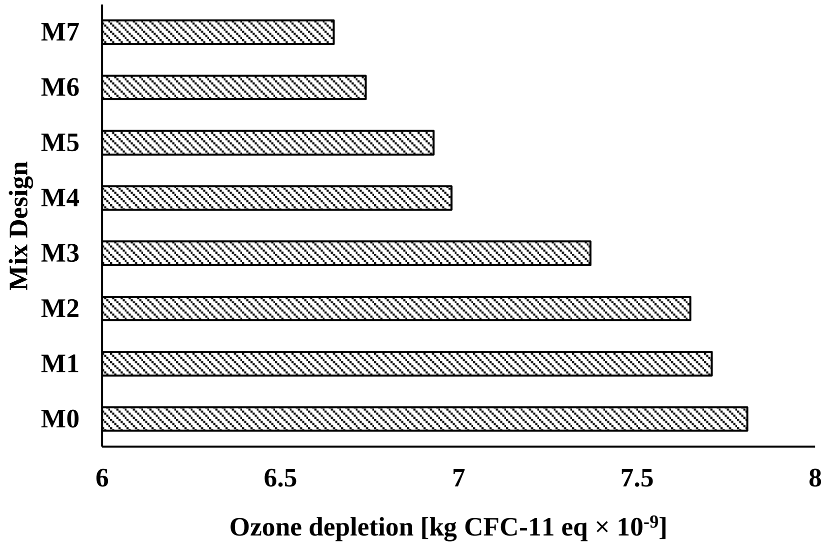

Figure 6.3: Impact of the ozone depletion

The effect of human toxicity due to the use of RHA-integrated mortar is shown in Table 6.2 as the equivalent of 1.4-dichlorobenzene (1.4-DB). Compared to Mo, the substitution of the mortar with RHA indicates that the sand replaced by RHA reduce the human toxicity maximum about 9%. Table 6.2 also shows the results of RHA substituted mortar for terrestrial acidification that are a predictor of the categories of SO2-related impacts. At the level of 30 % RHA in the mortar, the environmental impacts start to fall more by 7%. The lowest impact of terrestrial acidification is 100% of RHA replacement, which is 12.26 % lower than that of Mo (i.e. conventional mortar). The findings of the ecotoxicity of freshwater suggest that the RHA substitution is 30% to 70%, the environmental impact decreases more as 2.6% to 4%. The transportation distance to cement and RHA were most contributes to fossil fuels impact. By comparing with other raw materials, sand did not give much contribution to fossil depletion environmental impact as the transportation distance to sand is shorter than that of for other materials. Table 6.2 illustrates that the mix design M0 has the greatest effect on fossil depletion and the increase in the RHA replacement percentage reduces the effect of the depletion of fossil fuel. The optimum mix (i.e. 30% replacement of RHA) shows a reduction of 5% fossil fuel depletion than conventional mortar.

Overall, this LCA analysis highlights that increases in the RHA replacement in the mortar significantly reduced the environmental impact, which generates when producing cconventional mortar (Table 6.2). This indicates that the usage of the substituted products in different proportions is beneficial in the aspect of the environment. The 100% replacement of the sand with RHA gave the best results in respect to all the eight environmental impact categories taken for this LCA.

The construction process doesn't cease with the usage of the 1kg of the products. As the need of the mortar is huge, the usage of such kind of waste (RHA) incorporated products instead of traditional mortar, not only be an eco-friendly product but also gives economic and social benefits. Further, the physical and chemical study of RHA, which satisfies the requirement of ASTM C618 [66] as the RHA is categorized as type F pozzolans. The effectiveness of using the RHA in mortar as pozzolanic material was determined by subsequent tests.

This study observed that the addition of 30% of RHA by sand weight did not adversely affect the fresh and hardened mortar performance with the minimum compressive strength (i.e. 5.2 MPa) in compliance with standard ASTM C270. The mortar with 30% of RHA shows a 60% reduction of thermal conductivity and 14% reduction of greenhouse gas emission for 1 kg product.

Table 6.2: The results of Environmental impact

Mortar designation	Environmental impact categories			
	Human toxicity [kg 1,4-DB eq]	**Terrestrial acidification [kg SO_2 eq]**	**Freshwater ecotoxicity [kg 1,4-DB eq]**	**Fossil depletion [kg oil eq]**
M0	2.85E-01	1.55E-02	5.32E-03	2.96E-01
M1	2.82E-01	1.50E-02	5.21E-03	2.88E-01
M2	2.72E-01	1.48E-02	5.20E-03	2.87E-01
M3	2.69E-01	1.45E-02	5.18E-03	2.81E-01
M4	2.66E-01	1.42E-02	5.14E-03	2.78E-01
M5	2.64E-01	1.41E-02	5.11E-03	2.74E-01
M6	2.62E-01	1.38E-02	5.09E-03	2.73E-01
M7	2.60E-01	1.36E-02	5.08E-03	2.69E-01

CHAPTER 7: HEAT TRANSFER ANALYSIS

7.1 Overview

Further in order to examine the heat transfer mechanism of the RHA-based mortar plasters in the actual building profile, two prototype houses were built as shown in Figure 7.1a and plastered with conventional and RHA-based mortars. The model test houses were kept approximately 2 m apart from each other under open environment for 28 day after plaster applied on the wall. Heat transfer reduction was measured under open environmental conditions on the prototype model house. The width, length and height of the model houses were 750 mm, 900 mm and 750 mm, respectively and the thickness of wall was 100 mm. The model House A was used for control purpose, which has conventional plaster produced with the Mo mix and the model House B made up of RHA-based mortar with 30% of RHA content (i.e. M3 mix). Both model house plaster thickness was 20 mm.

Four K type thermocouples were located in the external and internal wall at locations $S_{E,}1$, $S_{E,}2$, $N_{E,}1$, and $N_{E,2}$ and $S_{I,}1$, $S_{I,}2$, $N_{I,}1$, and $N_{I,2}$ to measure the indoor and outdoor air and surface temperatures and recorded for 3 days as shown in Figure 7.1b. Field measurement data were gathered for 3 days during the month of August in the University of Moratuwa, situated in Colombo, the capital city of Sri Lanka, where the warm and cold temperature on the same day could be detected. A data logger was used to collect data for the duration of the test period at 1-min intervals over a 24-h period. The effect of radiation on the outer surface was assumed as same in both houses and there are no shadows of trees or building near the model houses (Figure 7.1c).

The representative wall surface temperature was derived via averaging the two temperatures in south and north direction measured on the outside (i.e. $S_{E,}1$, $S_{E,}2$, $N_{E,}1$, and $N_{E,2}$) and inside (i.e. $S_{I,}1$, $S_{I,}2$, $N_{I,}1$, and $N_{I,2}$). These temperatures were then used to derive the heat flux on the wall surface using Eq.1 by considering equilibrium of heat flow.

$$Q = \frac{K \times (T_{E-}T_{I})}{t} \qquad (1)$$

Where; Q is heat flux (W/m^2); K is overall thermal conductivity (W/m K); t is the wall thickness (m) and T_E and T_I are the external and internal wall surface average temperatures (ºC), respectively. The thermal conductivity of concrete block, conventional plaster (Mo mix) and RHA plaster (M3 mix) were taken as 1.4 W/m K, 0.81 W/m K and 0.33 W/m K, respectively [67].

(a)

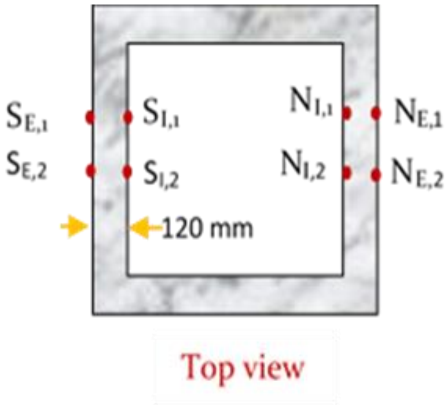

(b)

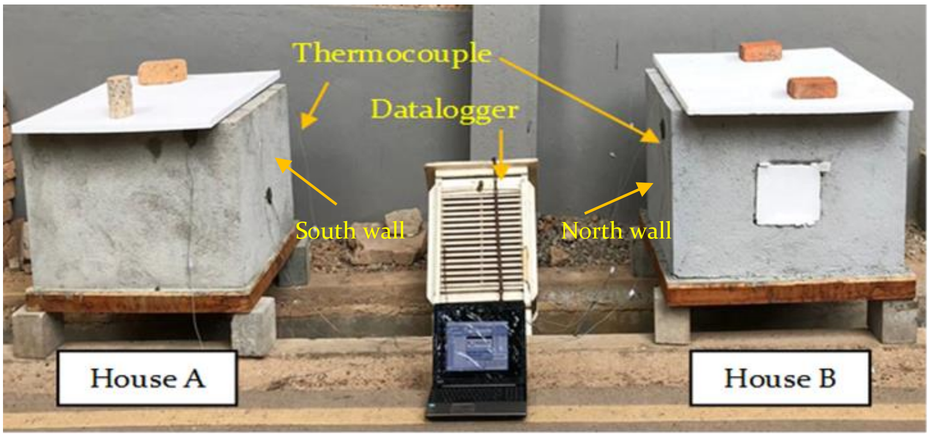

(c)

Figure 7.1: Test setup: (a) Test house construction; (b) location of thermocouples; and (c) test setup

7.2 Results and discussion

Figure 7.2 demonstrate the average temperatures on the outer ($S_{E,}1$, $S_{E,}2$, $N_{E,}1$, and $N_{E,2}$) and internal ($S_{I,}1$, $S_{I,}2$, $N_{I,}1$, and $N_{I,2}$) wall surface for a representative day. The outside surface temperature of the wall of both house a and b were similar with maximum variation of 0.05 ºC but the both internal surface temperature are varying with the external temperature and time (Figure 8). The temperature at inside the house is more than the environmental temperature at 13:00 pm (i.e. mid of the day), when applying conventional mortar plaster on the wall. Whilst, this inside temperature is about 12% lower than the environmental temperature in the house with RHA plaster wall. This indicates that RHA based plaster provide good thermal comfort for occupants. The thermal conductivity of House B' wall is lower than that of from House A and this was the reason the house B' wall produce relatively low internal surface temperature than the House A.

Further, Figure 7.2 shows that the internal surface temperature decreases more frequently and it's indicating that the cold quantity from indoor air has already been

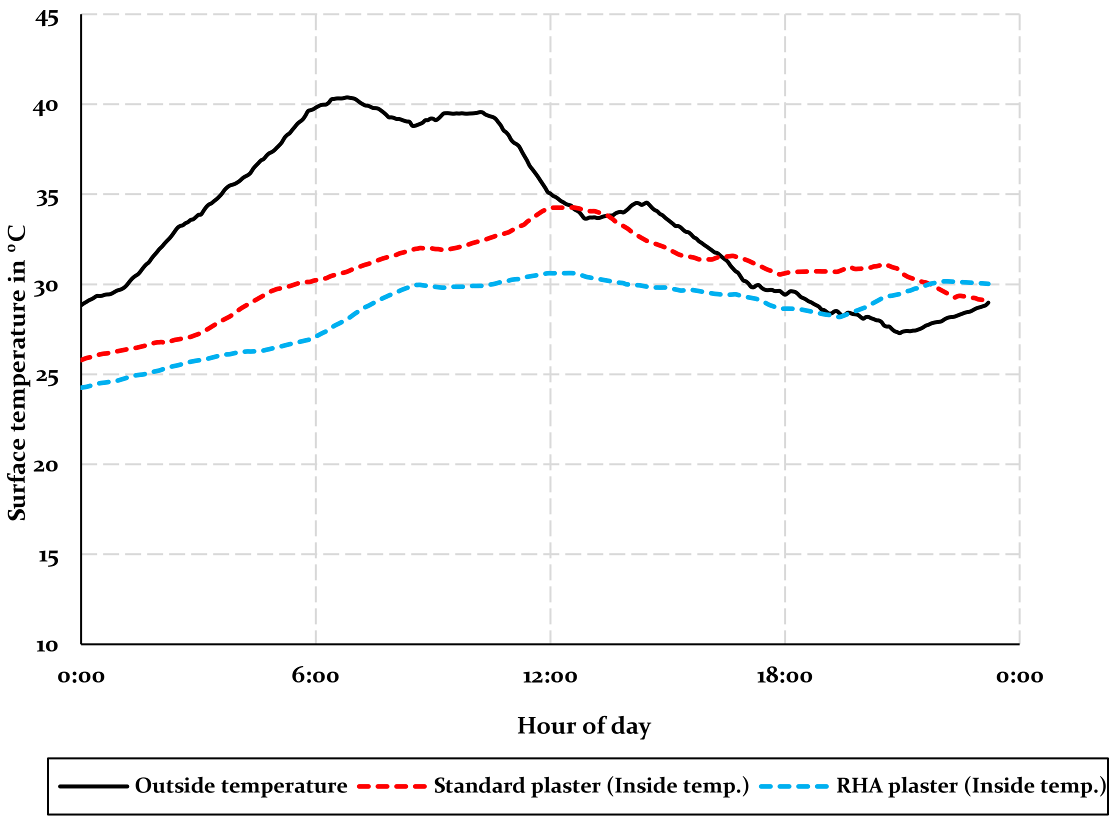

Figure 7.2: Outside and inside wall surface temperatures

retained by the walls. Further, the RHA-based mortar provides consistent indoor air temperature and wall surface temperatures, which would effectively offer greater thermal stability and greater occupant thermal comfort for occupants.

The heat fluxes for the walls derived for a representative day are shown in Figure 7.3. They highlight that compared to conventional mortar plaster wall, the peak heat flux decreased by an average of 10%, when the RHA-based plaster applied on the wall and, the average heat flux decreased by an average of 26%. This indicates that RHA-based plaster contributes significantly to reduce the wall heat flux and complete heat transfer into the conditioned room. Figure 7.3 also illustrates that higher heat fluxes were detected in the hours between 5 and 8 AM. During this period RHA-based plaster act as a good insulation layer, as the heat transfer and heat flux less than that of from the conventional plaster.

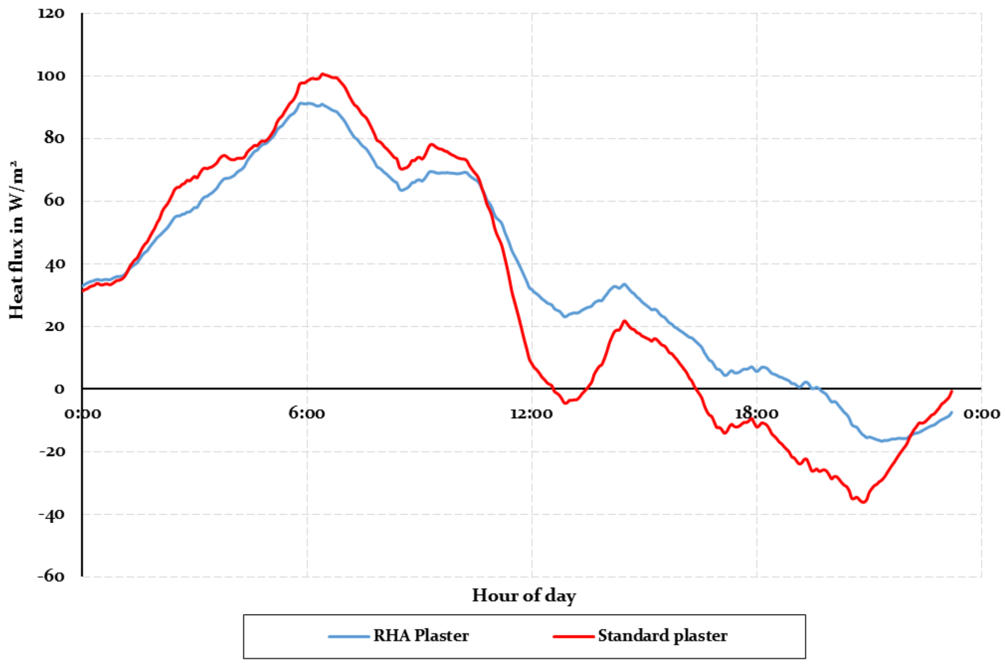

Figure 7.3: Wall heat fluxes

The average heat flux reduction over a 24-h period as detailed in Table 7.1. It also shows the total energy consumption at peak hour (daytime), which derived by the area under the heat flux vs time curve. Table 4 indicates that the house with RHA-based mortar plaster needs less energy to maintain the temperature comfort of the house than a house with conventional mortar plaster. Further, in the peak hour to maintain the thermal comfort of the house wall with RHA-based plaster consumed 9% less energy than the house with conventional wall plaster. Overall, experimental findings showed that the RHA-based plaster reduces the, heat flux, energy consumption and provide thermal comfort than the conventional plaster. This indicates that the RHA-based mortar is the sustainable option to reduce the operational energy consumption in the residential and commercial building. Especially for regional areas, where there is usually a major temperature fluctuation, the use of an RHA plastered wall will be an option to reduce the operational energy and related cost.

Table 7.1: Heat flux for daily cycles and total energy consumption at peak hour.

Date	**Average heat flux W/m^2**		**Total energy per unit area in peak hour kJ**	
	Standard plaster	**RHA plaster**	**Standard plaster**	**RHA plaster**
Day 1	36.7	28.9	291	270
Day 2	35.3	26	292	265
Day 3	33.9	23.1	296	268
Average	35.3	26	293	267
Difference % relative to standard plaster		26 %		9%

CHAPTER 8: TESTING RELATED TO CFRP AND INSULATION PLASTER

8.1 Overview

This chapter contains the results of the experiments regarding the CFRP and the above invented insulated thermal plaster. Tests regarding checking the thermal variations in the furnace using thermocouples in different temperature profiles using CFRP sheets and plaster were carried out

8.2 Thermal test

To check the performance of the plaster attached with CFRP sheets with the block size of 100 mm x 100 mm x 250 mm thermal fire test was carried out. First, specimens were sandblasted and CFRP sheets were pasted using adhesive in the concrete blocks as shown in Figure 9.3. After some hours developed plaster was applied on the top of the CFRP sheets with the thermocouples to check the temperature variation inside and outside the CFRP sheets as shown in Figure 8.1 and Figure 8.2.

Figure 8.1: CFRP sheets with cement block

Figure 8.2: CFRP blocks with plaster

Figure 8.3: Specimens with thermocouples

After 7 days, samples were tested using furnace with the temperature profile of room temperature to 500 °C as shown in Figure 8.4.

Figure 8.4: Testing setup

The temperature profile of an empty furnace is shown in Figure 8.5. To obtain temperature readings, the specimen was placed in the oven, and thermocouples were attached to a data logger. Every 10-sec interval reading was recorded in the data logger and through the computer, data were collected. Two samples were tested to get the average of the results. Figure 8.6 indicates the average temperature variance within the adhesive layer of each of the samples collected from two thermocouples for the block with normal plaster and plaster with RHA.

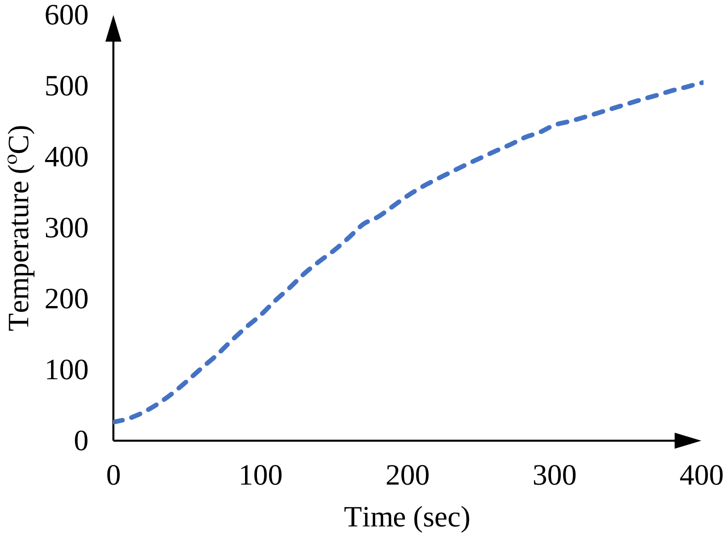

Figure 8.5: Temperature variation of furnace

From the results obtained in the test program, the time taken to reach the maximum temperature for RHA plaster is very less than the control plaster. It shows that RHA plaster has a good insulation property than conventional cement plaster.

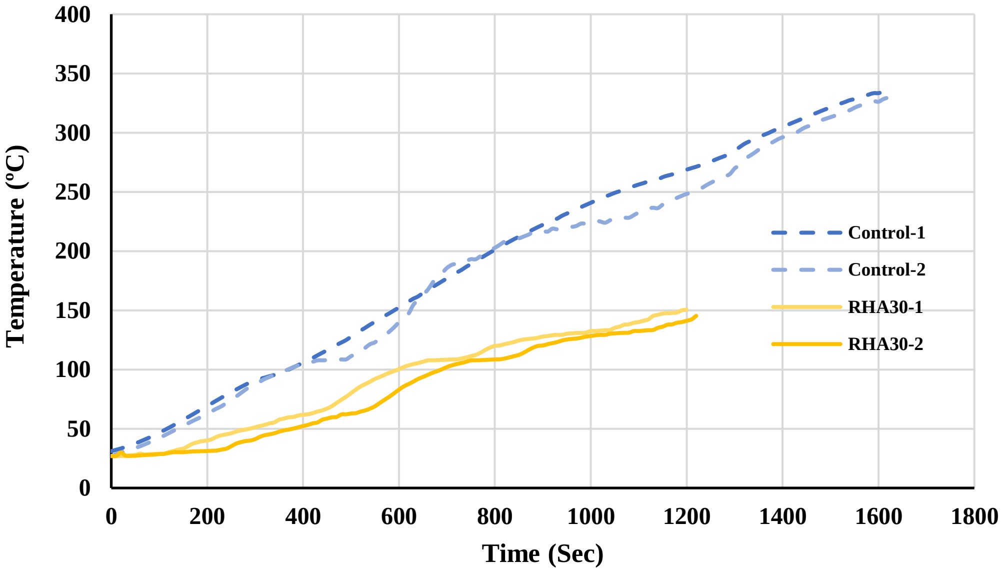

Figure 8.6: Temperature variation with time

8.3.1 Test setup

To check the performance of developed insulation layer concrete cylinder with the diameter of 100 mm and height of 200 mm were cast as shown in Figure 8.7. The compressive strength of cylinders is 25 MPa after 28 days of curing.

Figure 8.7: Concrete cylinder

After 28 days of curing, one-layer CFRP was wrapped around the surface of concrete cylinders as shown in Figure 8.8 with the help of adhesive.

Figure 8.8: Concrete cylinder wrapped with CFRP layer

After one day of exposure to open environment, the developed RHA plaster with the thickness of 30 mm was applied around the CFRP wrapped cylinders using epoxy as shown in Figure 8.9.

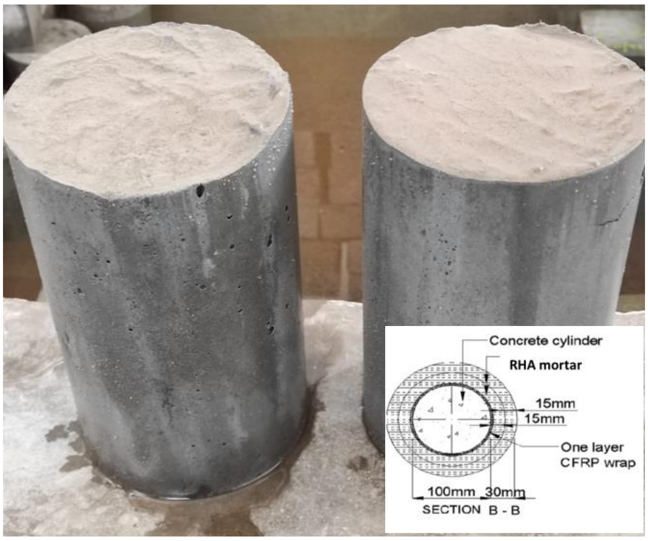

Figure 8.9: Concrete cylinder with CFRP wrapped with RHA plaster

After 28 days curing, the cylinders were subjected to heat treatment in furnace for 550 ºC (2 h exposure) and 715 ºC (2 h exposure).

8.3.2 Results

The heat treatment of the samples was carried out with and without thermal insulation. The table 8.1 shows the results of the heat treatment. All the results are average of two specimens.

Table 8.1: Test results of study

Test programme	Without thermal insulation Average Compressive strength at failure (MPa)	With thermal insulation Average Compressive strength at failure (MPa)
Control concrete cylinder (No CFRP wrap, No temperature exposure)	28	NA
Control concrete cylinder with 1-layer CFRP wrap	42.2	NA
Control concrete cylinder wrapped with 1-layer CFRP wrap and thereafter exposed to 550ºC (2 h)	19	26.2
Control concrete cylinder wrapped with 1-layer CFRP wrap and thereafter exposed to 715 ºC (2 h)	6.2 CFRP totally delaminated	14.952 CFRP completely delaminated

From the test results it was observed that RHA mortar with 30 mm thickness insulation is about 70 to 73% effective in protecting the concrete specimen with comparing with control one without exposed to temperature.

CHAPTER 9: CONCLUSION AND RECOMMENDATION

9.1 Conclusions

Two type of RHA (i.e., HRHA and LRHA) were used to produce the RHA-based mortar. The sustainability performance of RHA-based mortar in term of strength, cost, thermal properties, embodied energy and GHGE were studied. The following conclusions are drawn from the investigations.

- The compressive strength of both HRHA- and LRHA-based mortar was within the standard recommended range (~5.2 MPa) for mixtures with up to 30% RHA.
- Density of mortar was reduced, when increasing the RHA contents. This reduction was higher in the mortar with HRHA compared to the mortar containing LRHA.
- Thermal conductivity of mortar reduced with the increase of RHA replacement. The thermal conductivity of mortar containing 50% HRHA was about 72% and 22% lower than the conventional mortar and mortar with 50% LRHA, respectively. This indicates that increase of RHA content improve the thermal performance.
- Environmental impact assessment shows a significant reduction in embodied GHGE when mortar containing high volume of RHA. When the sand in the conventional mortar replaced with 30% HRHA reduced about 13% CO_2. This reduction was about 14.7% higher when 30% sand replaced with OBRHA in the conventional mortar mix. This was due to the energy intensive approach (i.e., furnace burning) used to produce the LRHA.
- The cost of control and LRHA-based mortar production is 6.5% and 18.5% higher than the HRHA-based mortar, respectively.

Overall, partially replacing sand with up to 30% of HRHA improved the thermal properties (i.e. lower thermal conductivity) and GHGE reduction with adequate compressive strength. This low thermal conductivity will enable the benefits to the operational energy (i.e. heating and cooling energy) building and reducing the carbon footprint. Thus, OBRHA has the potential to produce cost effective, environmentally friendly and energy efficient construction materials.

RHA mixed cement-based insulation plater was developed in order to reduce the cost of Insulation material. Since a huge amount of rice husk are available in the Country, this application would help to contribute reuse the waste materials. Thermal conductivity variation from 0.58 W/m K to 0.17 W/m K, compressive strength (28 days) variation from 14.44 MPa to 1.21 MPa, and density variation from 2050 Kg/m^3 to 1400 Kg/m^3 were noted from the test result.

RHA is one of the best waste materials which can be used for producing green building material. Pozzolan F type RHA can be successfully used to replace 30% of sand in conventional cementitious mortar. This may cause 41.7% of the decrease of dry density of mortar with respect to conventional mortar, result in reduced deadweight of walling units.

In the production process of insulation mortar for plastering using RHA, it is recommended to replace up to 30% of sand by RHA to produce type N mortar to comply with ASTM C270. RHA can be used to improve the thermal performance of cementitious materials. In the mortar production process, the thermal conductivity can be reduced up to 0.33 W/m K with a 30% RHA replacement. This may lead to the reduction of heat transfer through conduction by 60% which takes the lead towards energy savings in buildings. It is recommended to use cement: sand: RHA in the weight proportion of 1:2.1:0.9 with w/c ratio of 1.2 to produce mortar maintaining the balance between thermal and material properties while reducing the self-weight of the composite wall. LRHA and HRHA both can produce a very lightweight plaster. Both dry density and bulk density were less for LRHA than HRHA. Both LRHA and HRHA shows good thermal insulation property than conventional plaster; when compared both, LRHA shows good insulation property than HRHA.

In the case of compressive strength, LRHA satisfies the limit of ASTM C270 up to 30 % but for HRHA, it is about 20%. LRHA mortar shows good flowability than HRHA for a required water-cement ratio which means HRHA particles absorb more water than LRHA particles.

Environmental impact assessment highlighted that increasing RHA replacement for sand in the conventional mortar, reducing the climate change, ozone depletion, human toxicity, terrestrial acidification, freshwater ecotoxicity and fossil depletion.

The thermally enhanced RHA-based wall plaster improved the thermal control and enable better thermal comfort for occupants. As it produces the constant indoor air temperature and wall surface temperatures.

Heat transfer analysis indicated that plaster with 30% of RHA, reduced the peak heat flux by an average of 10% and average daily heat transfer by 26%.

In addition, testing was carried out to check the performance of CFRP with the above developed insulation plaster. Results showed a better profile for a thermal insulation system.

9.2 Recommendations

Sri Lanka is a green country which have a plenty of paddy cultivation. Therefore, using the RHA waste as a construction material is one of the sustainable method to reduce the environmental pollution. Overall, it can be concluded that the high-carbon RHA efficiency in terms of both strength and durability characteristics was less than the low-carbon RHA. Although past studies indicate that high-carbon concrete is not recommended due to unfavorable workability, using high-carbon RHA in the mortar mix indicates similar workability as low-carbon RHA. The insulated plaster produced in this research can be used in buildings as a wall plaster to improve thermal comfort, and an experimental program should be undertaken to test the practical feasibility of installing Material in wall panels. Cracking and spalling should be monitored on the plaster. Although the developed insulation material possesses good thermal and mechanical properties, its applicability should be tested on CFRP composites. In this case, the first suggestion would be to maintain the adhesion bond between the CFRP and the insulation. The thermal performance of Insulated CFRP composites should then be evaluated at elevated temperature or during fire.

REFERENCES

[1] P. Chotickai and S. Somana, "Performance of CFRP-Strengthened Concrete Beams after Exposure to Wet/Dry Cycles," *J. Compos. Constr.*, vol. 22, no. 6, pp. 1–10, 2018, doi: 10.1061/(ASCE)CC.1943-5614.0000895.

[2] J. Gamage, M. Wong, and R. Al-Mahaidi, "Durability of CFRP-Strengthened concrete members under extreme temperature and humidity," *Aust. J. Struct. Eng.*, vol. 9, no. 2, pp. 111–118, 2009, doi: 10.1080/13287982.2009.11465014.

[3] B. Gao, J. K. Kim, and C. K. Y. Leung, "Experimental study on RC beams with FRP strips bonded with rubber modified resins," *Compos. Sci. Technol.*, vol. 64, no. 16, pp. 2557–2564, 2004, doi: 10.1016/j.compscitech.2004.05.016.

[4] Y. K. Guruprasad and A. Ramaswamy, "Thermal insulation of concrete and the repair material CFRP exposed to high temperature and different time intervals," *Constr. Build. Mater.*, vol. 205, pp. 549–565, 2019, doi: 10.1016/j.conbuildmat.2019.01.236.

[5] J. P. Firmo and J. R. Correia, "Fire behaviour of thermally insulated RC beams strengthened with NSM-CFRP strips: Experimental study," *Compos. Part B Eng.*, vol. 76, pp. 112–121, 2015, doi: 10.1016/j.compositesb.2015.02.018.

[6] J. S. Patel, K. B. Parikh, and P. A. R. Darji, "Study on Concrete Using Fly Ash , Rise Husk Ash and Egg Shell Powder," vol. 5, no. Ii, pp. 566–570, 2017.

[7] M. N. Musa, M. Fikhri, and A. Aziz, "Thermal Conductivity for Mixture of Rice Husk Fiber and Gypsum," vol. 819, pp. 69–73, 2016, doi: 10.4028/www.scientific.net/AMM.819.69.

[8] J. C. P. H. Gamage, R. Al-Mahaidi, and M. B. Wong, "Bond characteristics of CFRP plated concrete members under elevated temperatures," *Compos. Struct.*, vol. 75, no. 1–4, pp. 199–205, 2006, doi: 10.1016/j.compstruct.2006.04.068.

[9] D. Kumar, M. Alam, P. X. W. Zou, J. G. Sanjayan, and R. A. Memon, "Comparative analysis of building insulation material properties and performance," *Renew. Sustain. Energy Rev.*, vol. 131, no. June, p. 110038, 2020, doi: 10.1016/j.rser.2020.110038.

[10] W. Food, *World Food and Agriculture*, vol. 274, no. 7102. 1959.

[11] S. Mayooran, S. Ragavan, and N. Sathiparan, "Comparative study on open air burnt low- and high-carbon rice husk ash as partial cement replacement in cement block production," *J. Build. Eng.*, vol. 13, no. May, pp. 137–145, 2017, doi: 10.1016/j.jobe.2017.07.011.

[12] A. L.O, Ettu;M.S.W. Mbajiorgu; K.C, Nwachukwu; J.I, "Variation of Strength of OPC-Rice Husk Ash Cement Composites with Water- Cement Ratio *1 ,3,4 2," vol. 2, no. 7, 2013.

[13] B. H. Abu Bakar, P. J. Ramadhansyah, and M. J. Megat Azmi, "Effect of rice husk ash fineness on the chemical and physical properties of concrete," *Mag. Concr. Res.*, vol. 63, no. 5, pp. 313–320, 2011, doi: 10.1680/macr.10.00019.

[14] S. K. Antiohos, V. G. Papadakis, and S. Tsimas, "Cement and Concrete Research Rice husk ash (RHA) effectiveness in cement and concrete as a function of reactive silica and fi neness," *Cem. Concr. Res.*, vol. 61–62, pp. 20–27, 2014, doi: 10.1016/j.cemconres.2014.04.001.

[15] S. K. Antiohos, V. G. Papadakis, and S. Tsimas, "Rice husk ash (RHA) effectiveness in cement and concrete as a function of reactive silica and fineness," *Cem. Concr. Res.*, vol. 61–62, pp. 20–27, 2014, doi: 10.1016/j.cemconres.2014.04.001.

[16] E. Mohseni, M. J. Kazemi, M. Koushkbaghi, B. Zehtab, and B. Behforouz, "Evaluation of mechanical and durability properties of fiber-reinforced lightweight geopolymer composites based on rice husk ash and nano-alumina," *Constr. Build. Mater.*, vol. 209, pp. 532–540, 2019, doi: 10.1016/j.conbuildmat.2019.03.067.

[17] M. Jamil, M. N. N. Khan, M. R. Karim, A. B. M. A. Kaish, and M. F. M. Zain, "Physical and chemical contributions of Rice Husk Ash on the properties of mortar," *Constr. Build. Mater.*, vol. 128, pp. 185–198, 2016, doi: 10.1016/j.conbuildmat.2016.10.029.

[18] E. Vasconcelos, S. Fernandes, J. L. Barroso De Aguiar, and F. Pacheco-Torgal, "Concrete retrofitting using metakaolin geopolymer mortars and CFRP," *Constr. Build. Mater.*, vol. 25, no. 8, pp. 3213–3221, 2011, doi: 10.1016/j.conbuildmat.2011.03.006.

[19] M. R. F. Gonc and C. P. Bergmann, "Thermal insulators made with rice husk ashes : Production and correlation between properties and microstructure," vol. 21, pp. 2059–2065, 2007, doi: 10.1016/j.conbuildmat.2006.05.057.

[20] R. Pode, "Potential applications of rice husk ash waste from rice husk biomass power plant," *Renew. Sustain. Energy Rev.*, vol. 53, pp. 1468–1485, 2016, doi: 10.1016/j.rser.2015.09.051.

[21] M. F. M. Zain, M. N. Islam, F. Mahmud, and M. Jamil, "Production of rice husk ash for use in concrete as a supplementary cementitious material," *Constr. Build. Mater.*, vol. 25, no. 2, pp. 798–805, 2011, doi: 10.1016/j.conbuildmat.2010.07.003.

[22] Y. Y. Kim, B. J. Lee, V. Saraswathy, and S. J. Kwon, "Strength and durability performance of alkali-activated rice husk ash geopolymer mortar," *Sci. World J.*, vol. 2014, 2014, doi: 10.1155/2014/209584.

[23] R. P. Jaya *et al.*, "Strength properties of rice husk ash concrete under sodium sulphate attack," *Int. J. Integr. Eng.*, vol. 10, no. 4, pp. 199–202, 2018.

[24] B. Singh, *Rice husk ash*. Elsevier Ltd, 2018.

[25] X. Liu, X. Chen, L. Yang, H. Chen, Y. Tian, and Z. Wang, "A review on recent advances in the comprehensive application of rice husk ash," *Res. Chem. Intermed.*, vol. 42, no. 2, pp. 893–913, 2016, doi: 10.1007/s11164-015-2061-y.

[26] H. Varshney, "Utilization of Rice Husk Ash in concrete as cement replacement," *IOSR J. Mech. Civ. Eng.*, vol. 01, no. 01, pp. 28–33, 2016, doi: 10.9790/1684-15010010128-33.

[27] C. L. Hwang, T. P. Huynh, and Y. Risdianto, "An application of blended fly

ash and residual rice husk ash for producing green building bricks," *J. Chinese Inst. Eng. Trans. Chinese Inst. Eng. A*, vol. 39, no. 7, pp. 850–858, 2016, doi: 10.1080/02533839.2016.1191376.

[28] S. Rukzon and P. Chindaprasirt, "Physical Properties of Cement Mortar Containing Waste Ash," *Appl. Mech. Mater.*, vol. 804, no. 325, pp. 129–132, 2015, doi: 10.4028/www.scientific.net/amm.804.129.

[29] P. Mishra, A. Chakraverty, and H. D. Banerjee, "Studies on physical and thermal properties of rice husk related to its industrial application," *J. Mater. Sci.*, vol. 21, no. 6, pp. 2129–2132, 1986, doi: 10.1007/BF00547958.

[30] S. Verma and M. Kumar, "Behaviour of fly ash and rice husk ash based geopolymer concrete," *Key Eng. Mater.*, vol. 775 KEM, pp. 596–602, 2018, doi: 10.4028/www.scientific.net/KEM.775.596.

[31] M. M. Ahmad, F. Ahmad, M. Azmi, and M. Z. A. Mohd Zahid, "Properties of Cement Mortar Consisting Raw Rice Husk," *Appl. Mech. Mater.*, vol. 802, pp. 267–271, 2015, doi: 10.4028/www.scientific.net/amm.802.267.

[32] G. G.S. and M. S. N., "Effect of PFA on Strength and Water Absorption of Mortar," *J. Civ. Eng. Sci. Technol.*, vol. 2, no. 1, pp. 7–11, 2011, doi: 10.33736/jcest.81.2011.

[33] M. Jamil, A. B. M. A. M. A. Kaish, S. N. Raman, and M. F. M. M. Zain, "Pozzolanic contribution of rice husk ash in cementitious system," *Constr. Build. Mater.*, vol. 47, no. May, pp. 588–593, 2013, doi: 10.1016/j.conbuildmat.2013.05.088.

[34] T. International and J. Of, "Experimental Study On Rice Husk As Fine Aggregates In Concrete," no. 1992, pp. 9–14, 2014.

[35] Z. Liu, Y. Ding, F. Wang, and Z. Deng, "Thermal insulation material based on SiO 2 aerogel," *Constr. Build. Mater.*, vol. 122, pp. 548–555, 2016, doi: 10.1016/j.conbuildmat.2016.06.096.

[36] S. Kofi, F. Kotoka, D. Mensah, and A. Kwame, "Investigation of the

compressive strength of pit sand , and sea sand mortar prisms produced with rice husk ash as additive,” *Constr. Build. Mater.*, vol. 151, pp. 383–387, 2017, doi: 10.1016/j.conbuildmat.2017.06.082.

[37] C. L. Hwang and T. P. Huynh, “Investigation into the use of unground rice husk ash to produce eco-friendly construction bricks,” *Constr. Build. Mater.*, vol. 93, no. 2015, pp. 335–341, 2015, doi: 10.1016/j.conbuildmat.2015.04.061.

[38] P. Chindaprasirt and S. Rukzon, “Strength, porosity and corrosion resistance of ternary blend Portland cement, rice husk ash and fly ash mortar,” *Constr. Build. Mater.*, vol. 22, no. 8, pp. 1601–1606, 2008, doi: 10.1016/j.conbuildmat.2007.06.010.

[39] P. Torkittikul, T. Nochaiya, and W. Wongkeo, “Utilization of coal bottom ash to improve thermal insulation of construction material,” *J. Mater. Cycles Waste Manag.*, 2015, doi: 10.1007/s10163-015-0419-2.

[40] R. Demirbog, “Influence of mineral admixtures on thermal conductivity and compressive strength of mortar,” *Energy Build.*, vol. 35, pp. 189–192, 2003.

[41] O. Na and Y. Xi, “Mechanical and durability properties of insulation mortar with rubber powder from waste tires,” *J. Mater. Cycles Waste Manag.*, 2016, doi: 10.1007/s10163-016-0475-2.

[42] A. K. Saha, P. K. Sarker, and V. Golovanevskiy, “Thermal properties and residual strength after high temperature exposure of cement mortar using ferronickel slag aggregate,” *Constr. Build. Mater.*, vol. 199, pp. 601–612, 2019, doi: 10.1016/j.conbuildmat.2018.12.068.

[43] V. Corinaldesi, A. Mazzoli, and R. Siddique, “Characterization of lightweight mortars containing wood processing by-products waste,” *Constr. Build. Mater.*, vol. 123, pp. 281–289, 2016, doi: 10.1016/j.conbuildmat.2016.07.011.

[44] A. Ghosh, A. Ghosh, and S. Neogi, “Reuse of fl y ash and bottom ash in mortars with improved thermal conductivity performance for buildings,” *Heliyon*, no. September, p. e00934, 2018, doi: 10.1016/j.heliyon.2018.e00934.

[45] B. Ayobami and C. Dai, “Development of banana fibers and wood bottom ash modified cement mortars,” *Constr. Build. Mater.*, vol. 241, p. 118041, 2020, doi: 10.1016/j.conbuildmat.2020.118041.

[46] N. Benmansour, B. Agoudjil, A. Gherabli, A. Kareche, and A. Boudenne, “Thermal and mechanical performance of natural mortar reinforced with date palm fibers for use as insulating materials in building,” *Energy Build.*, vol. 81, pp. 98–104, 2014, doi: 10.1016/j.enbuild.2014.05.032.

[47] M. G. Gomes, I. Flores-Colen, F. da Silva, and M. Pedroso, “Thermal conductivity measurement of thermal insulating mortars with EPS and silica aerogel by steady-state and transient methods,” *Constr. Build. Mater.*, vol. 172, pp. 696–705, 2018, doi: 10.1016/j.conbuildmat.2018.03.162.

[48] T. B. Carlos, J. P. C. Rodrigues, R. C. A. de Lima, and D. Dhima, “Experimental analysis on flexural behaviour of RC beams strengthened with CFRP laminates and under fire conditions,” *Compos. Struct.*, vol. 189, pp. 516–528, 2018, doi: 10.1016/j.compstruct.2018.01.094.

[49] ASTM C 1437-07, “Standard Test Method for Flow of Hydraulic Cement Mortar,” *Annu. B. ASTM Stand.*, pp. 6–7, 2009.

[50] ASTM Committee, “ASTM C109/C109M-02 Standard Test Method for Compressive Strength of Hydraulic Cement Mortars,” *Annu. B. ASTM Stand.*, vol. 04, pp. 1–6, 2002, doi: 10.1520/C0109.

[51] I. Kett, “Compressive Strength of Hydraulic Cement Mortars (C 109),” *Eng. Concr.*, pp. 29–31, 2009, doi: 10.1201/9781420091175-c5.

[52] J. C. Mendes *et al.*, “On the relationship between morphology and thermal conductivity of cement-based composites,” *Cem. Concr. Compos.*, vol. 104, no. October 2018, p. 103365, 2019, doi: 10.1016/j.cemconcomp.2019.103365.

[53] A. S. Gill and R. Siddique, “Strength and micro-structural properties of self-compacting concrete containing metakaolin and rice husk ash,” *Constr. Build. Mater.*, vol. 157, pp. 51–64, 2017, doi: 10.1016/j.conbuildmat.2017.09.088.

[54] J. MacMullen, Z. Zhang, E. Rirsch, H. N. Dhakal, and N. Bennett, "Brick and mortar treatment by cream emulsion for improved water repellence and thermal insulation," *Energy Build.*, vol. 43, no. 7, pp. 1560–1565, 2011, doi: 10.1016/j.enbuild.2011.02.014.

[55] S. M. S. Kazmi, S. Abbas, M. J. Munir, and A. Khitab, "Exploratory study on the effect of waste rice husk and sugarcane bagasse ashes in burnt clay bricks," *J. Build. Eng.*, vol. 7, pp. 372–378, 2016, doi: 10.1016/j.jobe.2016.08.001.

[56] S. Abbas, S. M. S. Kazmi, and M. J. Munir, "Potential of rice husk ash for mitigating the alkali-silica reaction in mortar bars incorporating reactive aggregates," *Constr. Build. Mater.*, vol. 132, pp. 61–70, 2017, doi: 10.1016/j.conbuildmat.2016.11.126.

[57] ASTM C 270-07, "Standard Specification for Mortar for Unit Masonry," *United States Am. Soc. Test. Mater.*, pp. 2–13, 2007, doi: 10.1520/C0270-14A.Copyright.

[58] A. Shenoy, S. Kumar, A. Tantri, and A. Lakshmi, "STUDY OF STATIC AND DYNAMIC MODULUS OF ELASTICITY OF UHPC WITH AND WITHOUT COARSE AGGREGATES," no. June, pp. 2425–2430, 2018.

[59] H. Lime, M. Cabinets, and M. Rooms, "Standard Specification for Mortar for Unit Masonry 1," pp. 1–14, 2017, doi: 10.1520/C0270-14A.Copyright.

[60] M. Goedkoop, M. Oele, J. Leijting, T. Ponsioen, and E. Meijer, "Introduction to LCA with SimaPro Colophon," *Introd. to LCA with SimaPro*, no. November, 2016.

[61] A. Jayalath, S. Navaratnam, T. Ngo, P. Mendis, N. Hewson, and L. Aye, "Life cycle performance of Cross Laminated Timber mid-rise residential buildings in Australia," *Energy Build.*, vol. 223, p. 110091, 2020, doi: 10.1016/j.enbuild.2020.110091.

[62] S. Pushkar, "The effect of different concrete designs on the life-cycle assessment of the environmental impacts of concretes containing furnace

bottom-ash instead of sand," *Sustain.*, vol. 11, no. 15, 2019, doi: 10.3390/su11154083.

[63] F. Colangelo, A. Forcina, I. Farina, and A. Petrillo, "Life Cycle Assessment (LCA) of different kinds of concrete containing waste for sustainable construction," *Buildings*, vol. 8, no. 5, 2018, doi: 10.3390/buildings8050070.

[64] Standards Australia, "Standard Australia, Environmental management - Life cycle assessment - Principles and framework in: AS ISO 14040, Australia, 2019," *Stand. Aust. Environ. Manag. - Life cycle Assess. - Princ. Framew. AS ISO 14040, Aust. 2019*, 2019, [Online]. Available: https://infostore.saiglobal.com/en-us/Standards/AS-ISO-14040-2019-1153344_SAIG_AS_AS_2737699/.

[65] "BSI, Sustainability of construction works - Assessment of environmental performance of buildings," 2012, [Online]. Available: https://www.en-standard.eu/bs-en-15978-2011-sustainability-of-construction-works-assessment-of-environmental-performance-of-buildings-calculation-method/.

[66] Astm, "Standard Specification for Coal Fly Ash and Raw or Calcined Natural Pozzolan for Use," *Annu. B. ASTM Stand.*, no. C, pp. 3–6, 2010, doi: 10.1520/C0618.

[67] Y. Qu, J. Chen, L. Liu, T. Xu, H. Wu, and X. Zhou, "Study on properties of phase change foam concrete block mixed with paraffin / fumed silica composite phase change material," *Renew. Energy*, vol. 150, pp. 1127–1135, 2020, doi: 10.1016/j.renene.2019.10.073.

APPENDIX A

A.1: Invented product- AGRO MORTAR

AGRO MORTAR

Advanced modified cementitious sustainable light weight, thermal insulating masonry mortar

Product Description

Agro Mortar is prepared by blending Ordinary Portland cement with Rice Husk Ash (10-50 μm) and Fine aggregates (0.25-1.18 mm).
Very light weight plaster
High thermal insulation plaster
Grey in colour.
RHA Mortar meets the requirements of a category Type N mortar according to ASTM C270.

Advantages

Only water adding is the process to make the plaster
Easy to apply
Can be use in both wet and dry condtion

Instructions ForUse

Mixes the product using mechanical mixer for the better mixer.
Adding the water in the appropriate manner.
More addition water tends to reduce the strength

Technical Data

Agro Mortar	Typical Values @ 25°C
Appearance	Grey colour Powder
Max aggregate size	2 mm
Application thickness	10 - 30 mm
Dry hardened density	980 kg/m^3
Wet density	1600 kg/m^3
Pot life @ 25˚C	2.5 Hours Approx.
Compressive strength @ 28 day	5-10 MPa
Thermal conductivity	0.2-0.3 W/m K
Flow	130-140 mm
Water Absorption	≤ 0.85 kg/m^2

Technical Data Sheet- Agro Mortar

A.2: DATA FOR PHYSICAL PROPERTIES

A.2.1: Sieve analysis

Table A.1: Sieve analysis data

SIEVE ANALYSIS DATA							
Sieve Size (mm)	**Sand**			**High-carbon RHA**		**Low -carbon RHA**	
	passing through sieve	Percentage finer		passing through sieve	Percentage finer	passing through sieve	Percentage finer
5.00	2105.00	97.91		395.00	100.00	400.00	100.00
4.75	2075.00	96.51		395.00	100.00	400.00	100.00
2.36	1960.00	91.16		395.00	100.00	400.00	100.00
1.70	1810.00	84.19		395.00	100.00	364.00	090.87
1.18	1545.00	71.86		390.00	098.73	335.00	083.54
0.60	0605.00	28.14		355.00	089.87	249.00	062.03
0.43	0265.00	12.33		300.00	075.95	198.00	049.37
0.30	0070.00	03.26		235.00	059.49	132.00	032.91
0.15	0000.00	00.00		115.50	029.24	031.00	007.59
0.08	0000.00	00.00		040.00	010.13	000.00	000.00
0.00	0000.00	00.00		000.00	000.00	000.00	000.00

A.2.2: Chemical Composition

Table A.2: Chemical composition data of LRHA and HRHA

	Low carbon RHA	High carbon RHA
SiO2	81.4	51.2
Al_2O_3	1.10	0.3
Fe_2O_3	0.70	0.3
CaO	2.60	2.8
MgO	1.10	1.4
Na_2O	0.30	0.8
K_2O	0.60	3.4
SO_3	0.96	0.68
LOI	2.8	39.12

A.2.3: Density

Table A.3: Density data of LRHA and HRHA

Low carbon RHA				
Specimen	Dry weight (kg)	Dry density (kg/m^3)	Saturated weight (kg), (W_1)	Bulk density (kg/m^3)
RHA10-1	0.571	1738.156	0.682	2046.388
RHA10-2	0.582	1771.640	0.681	2043.388
RHA10-3	0.578	1759.464	0.679	2037.387
RHA20-1	0.496	1509.852	0.628	1884.358
RHA20-2	0.493	1500.719	0.625	1875.356
RHA20-3	0.500	1522.028	0.698	2094.397

RHA30-1	0.423	1287.635	0.585	1755.333
RHA30-2	0.421	1281.547	0.584	1752.332
RHA30-3	0.435	1324.164	0.579	1737.330
RHA50-1	0.316	961.921	0.528	1584.301
RHA50-2	0.318	968.010	0.521	1563.297
RHA50-3	0.323	983.230	0.526	1578.299
RHA70-1	0.248	754.926	0.473	1419.269
RHA70-2	0.242	736.661	0.476	1428.271
RHA70-3	0.254	773.190	0.475	1425.270
RHA80-1	0.231	703.177	0.465	1395.265
RHA80-2	0.235	715.353	0.462	1386.263
RHA80-3	0.245	745.793	0.460	1380.262
RHA100-1	0.193	587.502	0.430	1290.245
RHA100-2	0.198	602.723	0.425	1275.242
RHA100-3	0.189	575.326	0.431	1293.245

High carbon RHA				
Specimen	Dry weight (kg)	Dry density (kg/m^3)	Saturated weight (kg), (W_1)	Bulk density (kg/m^3)
RHA10-1	0.623	1896.447	0.749	2280.477
RHA10-2	0.645	1963.416	0.771	2347.460
RHA10-3	0.651	1981.680	0.777	2365.728
RHA20-1	0.545	1659.010	0.671	2042.991
RHA20-2	0.542	1649.878	0.668	2033.857
RHA20-3	0.539	1640.746	0.665	2024.722
RHA30-1	0.501	1525.072	0.627	1909.024
RHA30-2	0.511	1555.512	0.637	1939.471
RHA30-3	0.509	1549.424	0.635	1933.382
RHA50-1	0.412	1254.151	0.538	1638.046

RHA50-2	0.411	1251.107	0.537	1635.001
RHA50-3	0.408	1241.975	0.534	1625.867
RHA70-1	0.301	916.261	0.427	1300.085
RHA70-2	0.312	949.745	0.438	1333.576
RHA70-3	0.309	940.613	0.435	1324.442
RHA80-1	0.286	870.600	0.412	1254.414
RHA80-2	0.285	867.556	0.411	1251.370
RHA80-3	0.283	861.468	0.409	1245.280
RHA100-1	0.222	675.780	0.348	1059.554
RHA100-2	0.218	663.604	0.344	1047.375
RHA100-3	0.232	706.221	0.358	1090.001

A.2.4: Water absorption

Table A.4: Water Absorption data of LRHA and HRHA

Low carbon RHA				
Specimen	Saturated weight (kg), (W_1)	Dry weight (kg), (W_2)	Absorbed water (kg)	Water absorption rate (%)
RHA10-1	0.682	0.571	0.111	19.4
RHA10-2	0.681	0.582	0.099	17.01
RHA10-3	0.679	0.578	0.101	17.47
RHA20-1	0.628	0.496	0.132	26.6
RHA20-2	0.625	0.493	0.132	26.77
RHA20-3	0.698	0.500	0.198	39.60
RHA30-1	0.585	0.423	0.162	38.29
RHA30-2	0.584	0.421	0.163	38.71
RHA30-3	0.579	0.435	0.144	33.10
RHA50-1	0.528	0.316	0.212	67.08

RHA50-2	0.521	0.318	0.203	63.83
RHA50-3	0.526	0.323	0.203	62.84
RHA70-1	0.473	0.248	0.225	90.72
RHA70-2	0.476	0.242	0.234	96.69
RHA70-3	0.475	0.254	0.221	87.00
RHA80-1	0.465	0.231	0.234	101.29
RHA80-2	0.462	0.235	0.227	96.59
RHA80-3	0.460	0.245	0.215	87.75
RHA100-1	0.430	0.193	0.237	122.79
RHA100-2	0.425	0.198	0.227	114.64
RHA100-3	0.431	0.189	0.242	128.04

High carbon RHA				
Specimen	Saturated weight (kg), (W_1)	Dry weight (kg), (W_2)	Absorbed water (kg)	Water absorption rate (%)
RHA10-1	0.749	0.623	0.100	19.40
RHA10-2	0.771	0.645	0.099	17.01
RHA10-3	0.777	0.651	0.101	17.47
RHA20-1	0.671	0.545	0.132	26.60
RHA20-2	0.668	0.542	0.132	26.77
RHA20-3	0.665	0.539	0.198	39.60
RHA30-1	0.627	0.501	0.162	38.29
RHA30-2	0.637	0.511	0.163	38.71
RHA30-3	0.635	0.509	0.144	33.10
RHA50-1	0.538	0.412	0.212	67.08
RHA50-2	0.537	0.411	0.203	63.83
RHA50-3	0.534	0.408	0.203	62.84

RHA70-1	0.427	0.301	0.225	90.72
RHA70-2	0.438	0.312	0.234	96.69
RHA70-3	0.435	0.309	0.221	87.00
RHA80-1	0.412	0.286	0.234	101.29
RHA80-2	0.411	0.285	0.227	96.59
RHA80-3	0.409	0.283	0.215	87.75
RHA100-1	0.348	0.222	0.237	122.79
RHA100-2	0.344	0.218	0.227	114.64
RHA100-3	0.358	0.232	0.242	128.04

APPENDIX B

B.1: DATA FOR MECHANICAL PROPERTIES

B.1.1: Compressive Strength

Table B.1: Compressive strength at 7 days

Low carbon RHA			
Percentage (%)	No	Compressive strength (MPa)	Avg. compressive strength (MPa)
0	1	16.24	
	2	16.10	
	3	16.86	16.4
10	1	8.23	
	2	8.25	
	3	8.36	8.21
20	1	6.63	
	2	6.52	
	3	6.66	6.52
30	1	4.32	
	2	4.36	
	3	4.23	4.31
50	1	3.63	
	2	3.78	1.61
	3	3.65	
70	1	2.82	
	2	2.78	2.83
	3	2.89	
80	1	1.62	1.62

	2	1.68	
	3	1.58	
100	1	0.82	0.86
	2	0.91	
	3	0.86	

High carbon RHA			
Percentage (%)	No	Compressive strength (MPa)	Avg. compressive strength (MPa)
0	1	16.24	16.4
	2	16.10	
	3	16.86	
10	1	8.01	8.05
	2	8.04	
	3	8.10	
20	1	5.88	5.78
	2	5.66	
	3	5.82	
30	1	3.88	3.84
	2	3.86	
	3	3.78	
50	1	2.31	2.34
	2	2.34	
	3	2.38	
70	1	1.88	1.88

	2	1.92	
	3	1.86	
80	1	0.98	1.01
	2	1.02	
	3	1.03	
100	1	0.56	0.34
	2	0.48	
	3	0.52	

Table B.2: Compressive strength at 28 days

Low carbon RHA			
Percentage (%)	No	Compressive strength (MPa)	Avg. compressive strength (MPa)
0	1	22.63	
	2	22.62	
	3	22.58	22.61
10	1	14.44	
	2	14.42	
	3	14.53	14.42
20	1	8.24	
	2	8.26	
	3	8.18	8.22
30	1	5.86	
	2	5.82	
	3	5.90	5.86
50	1	4.85	4.84

	2	4.80	
	3	4.88	
70	1	3.21	3.21
	2	3.25	
	3	3.18	
80	1	2.17	2.17
	2	2.15	
	3	2.20	
100	1	1.21	1.25
	2	1.23	
	3	1.28	

High carbon RHA			
Percentage (%)	No	Compressive strength (MPa)	Avg. compressive strength (MPa)
0	1	22.63	22.61
	2	22.62	
	3	22.58	
10	1	13.44	13.41
	2	13.42	
	3	13.53	
20	1	7.21	7.21
	2	7.23	
	3	7.15	
30	1	4.80	4.82

	2	4.85	
	3	4.81	
50	1	3.86	3.81
	2	3.80	
	3	3.88	
70	1	3.01	3.01
	2	3.02	
	3	2.98	
80	1	1.88	1.84
	2	1.86	
	3	1.84	
100	1	1.01	1.02
	2	0.98	
	3	1.10	

B.1.2: Thermal Conductivity

Table B.3: Thermal conductivity

Low carbon RHA			
Percentage (%)	No	Thermal conductivity	Avg. thermal conductivity
0	1	0.824	0.846
	2	0.868	
10	1	0.584	0.555
	2	0.526	

20	1	0.402	0.444
	2	0.485	
30	1	0.310	0.354
	2	0.398	
50	1	0.282	0.280
	2	0.278	
70	1	0.174	0.170
	2	0.166	
80	1	0.146	0.141
	2	0.136	
100	1	0.132	0.127
	2	0.122	